Outline: Radiation emission

Lecturer: Hans-Jürgen Wollersheim

e-mail: h.j.wollersheim@gsi.de

web-page: https://web-docs.gsi.de/~wolle/ and click on

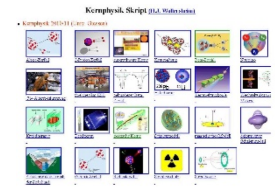

1. photons in the universe
2. nuclear resonance fluorescence
3. synchrotron radiation
4. wiggler and undulator
5. inverse Compton scattering

Photons in the universe

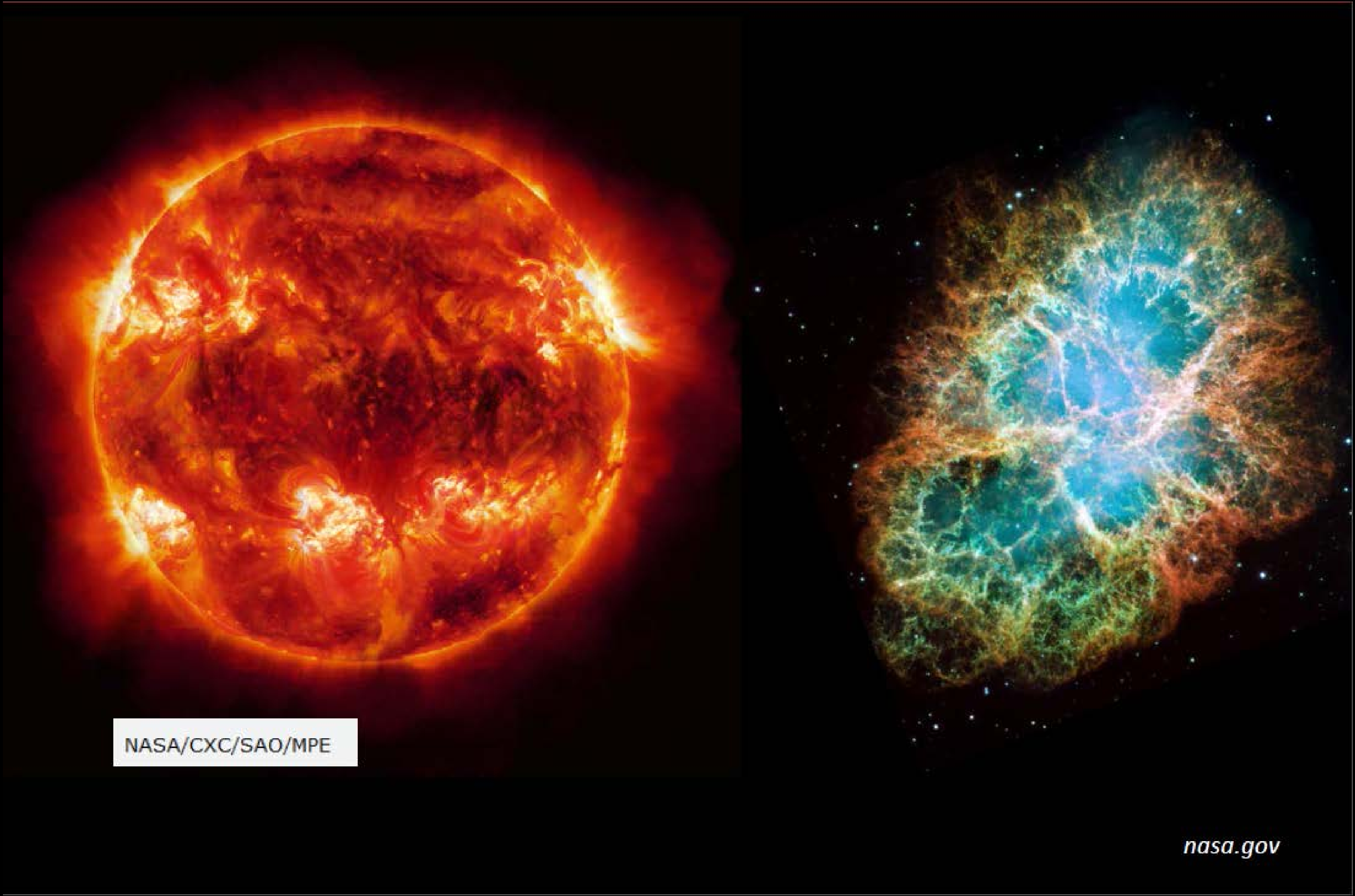

Photons in the universe

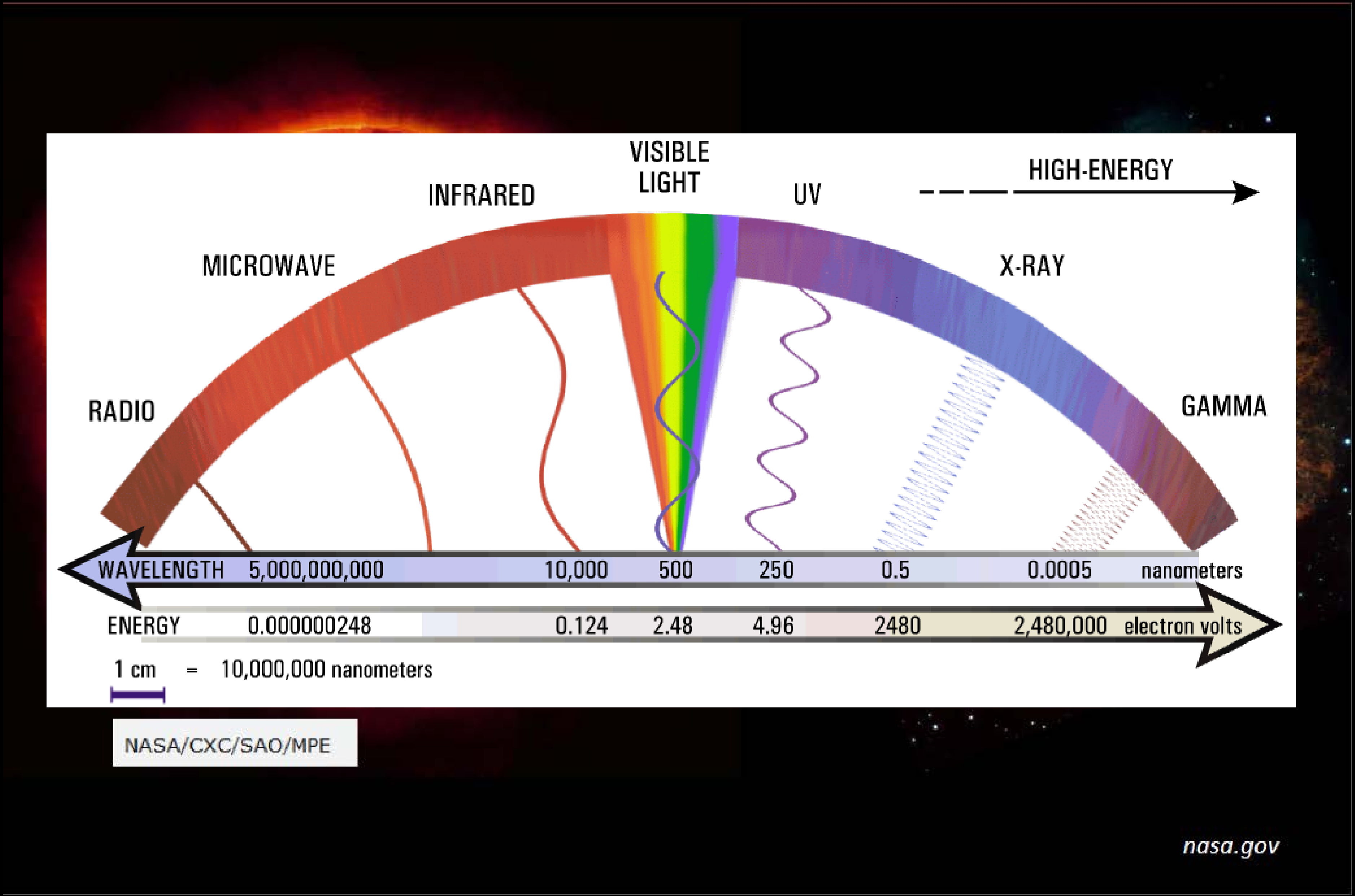

Element production on the sun

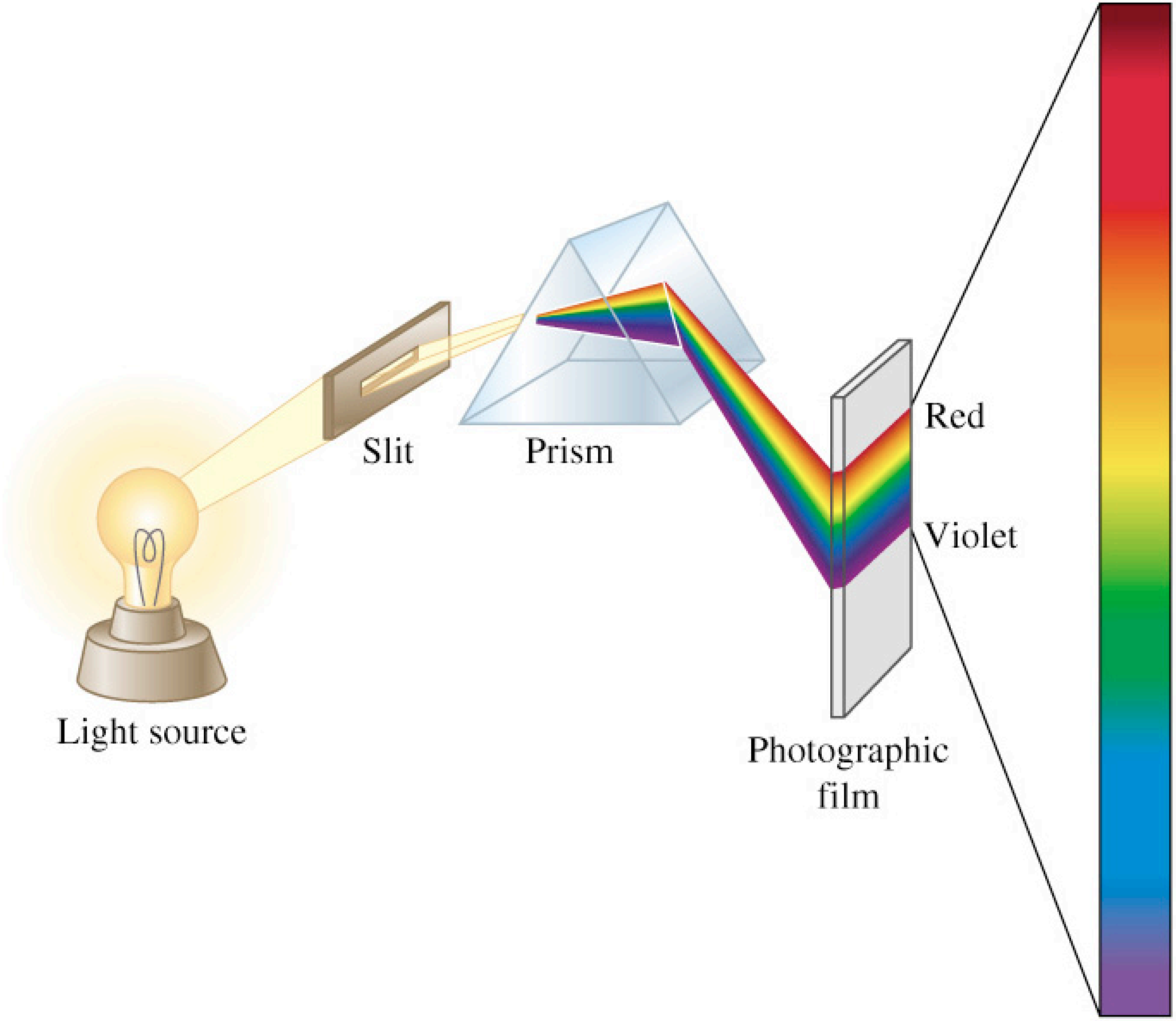

Spectral lines of hydrogen

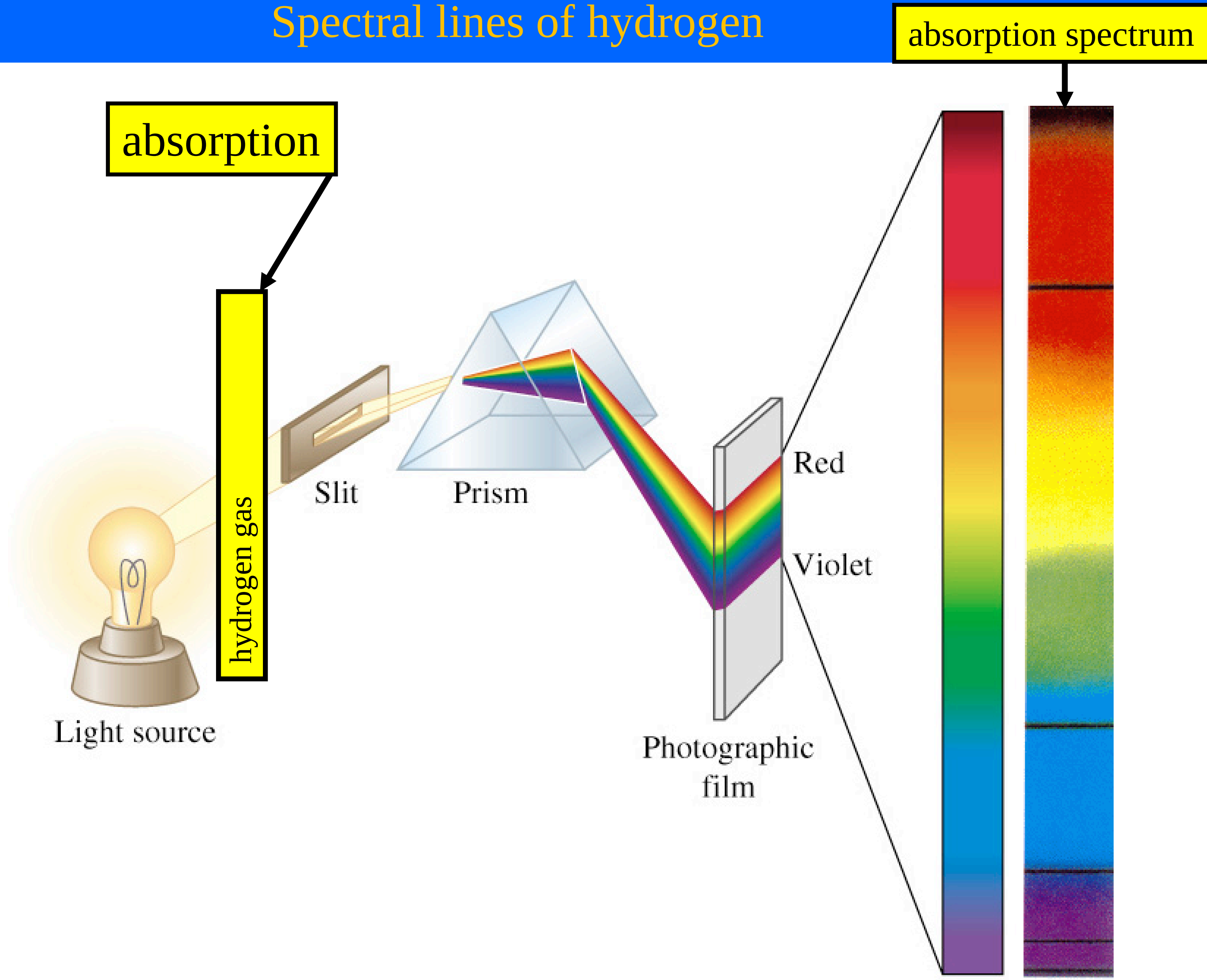

Hydrogen emission spectrum

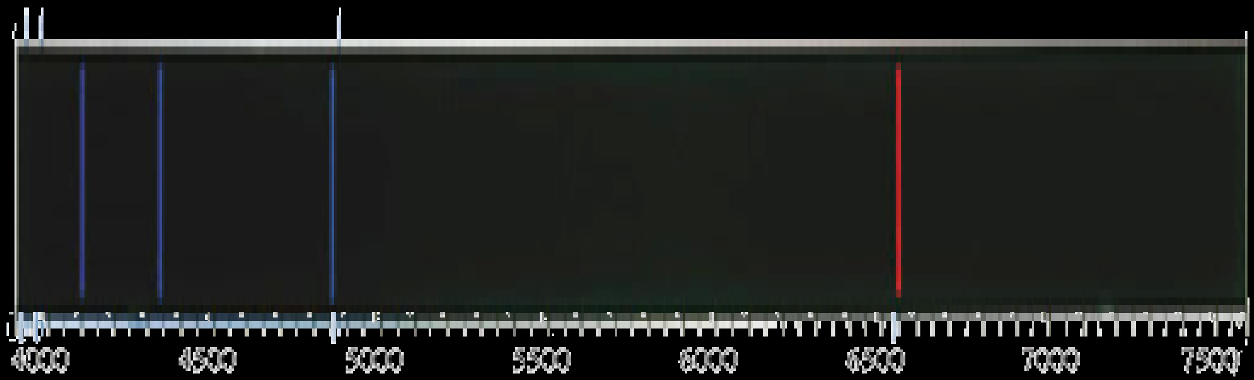

wave length nm

Spectral analysis

H

Spectral analysis
Kirchhoff und Bunsen:
Every element has a characteristic emission band

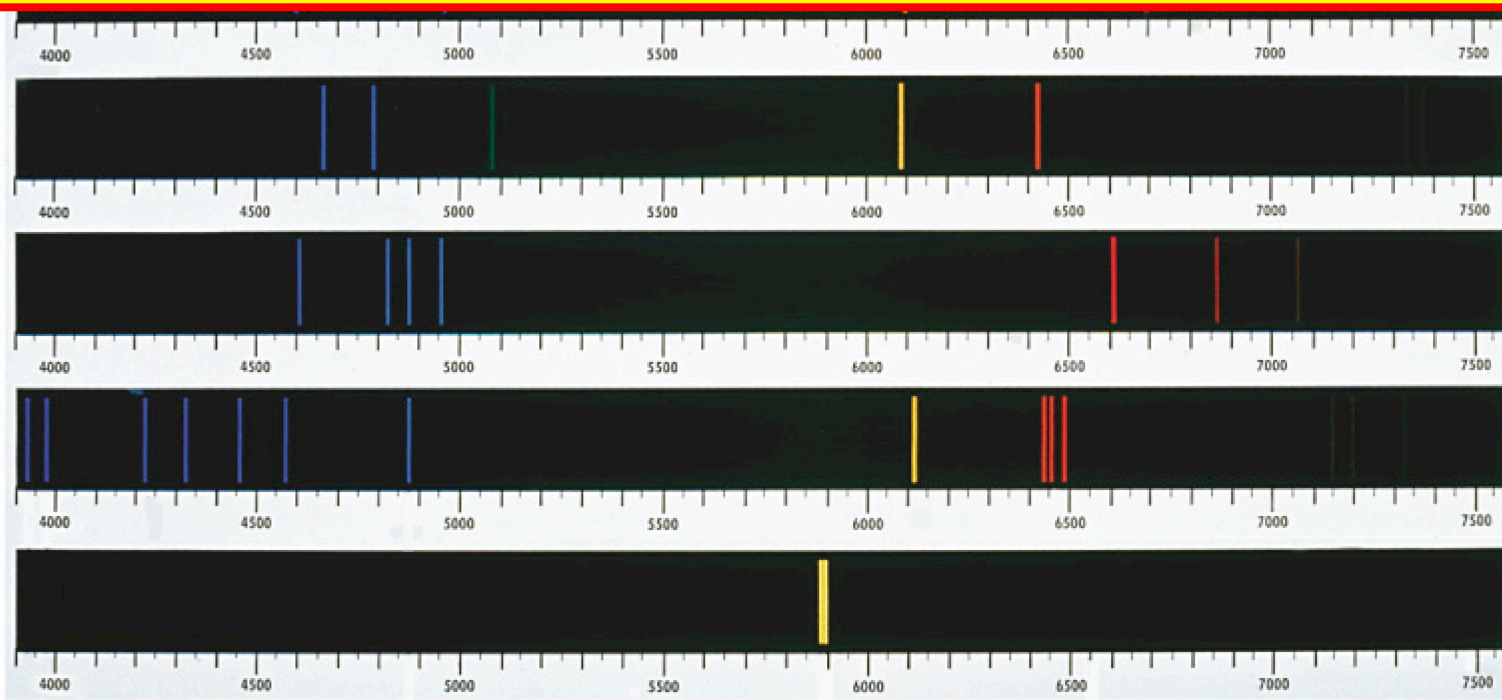

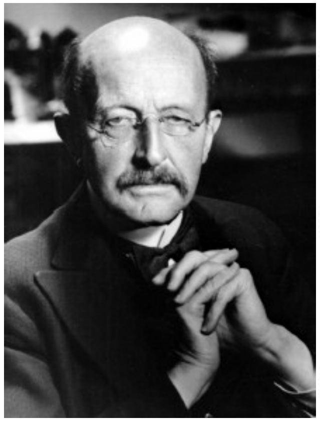

Max Planck

Nuclear Resonance Fluorescence

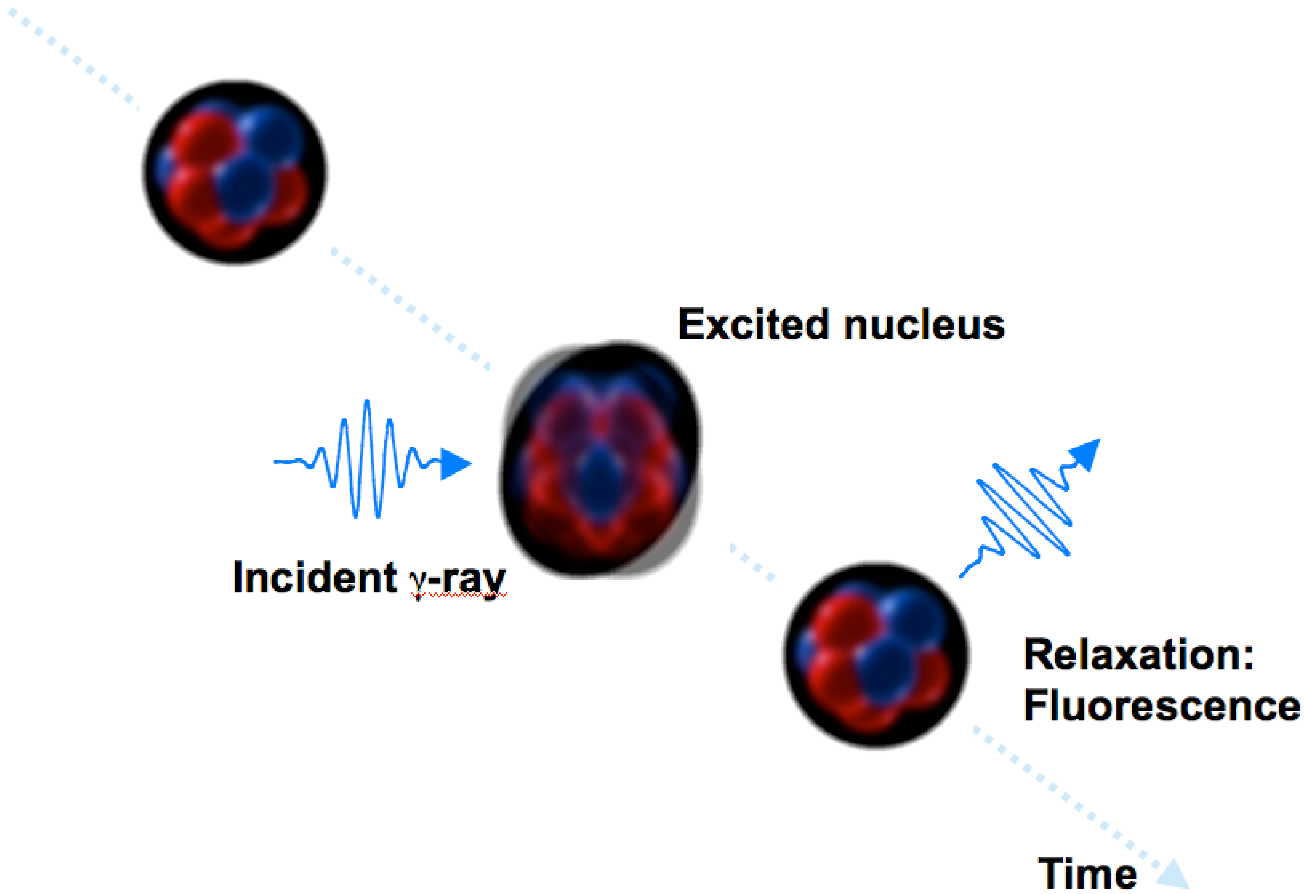

Nuclear Resonance Fluorescence (NRF) is analogous to atomic resonance fluorescence but depends upon the number of protons AND the number of neutrons in the nucleus

Low energy photon scattering at S-DALINAC

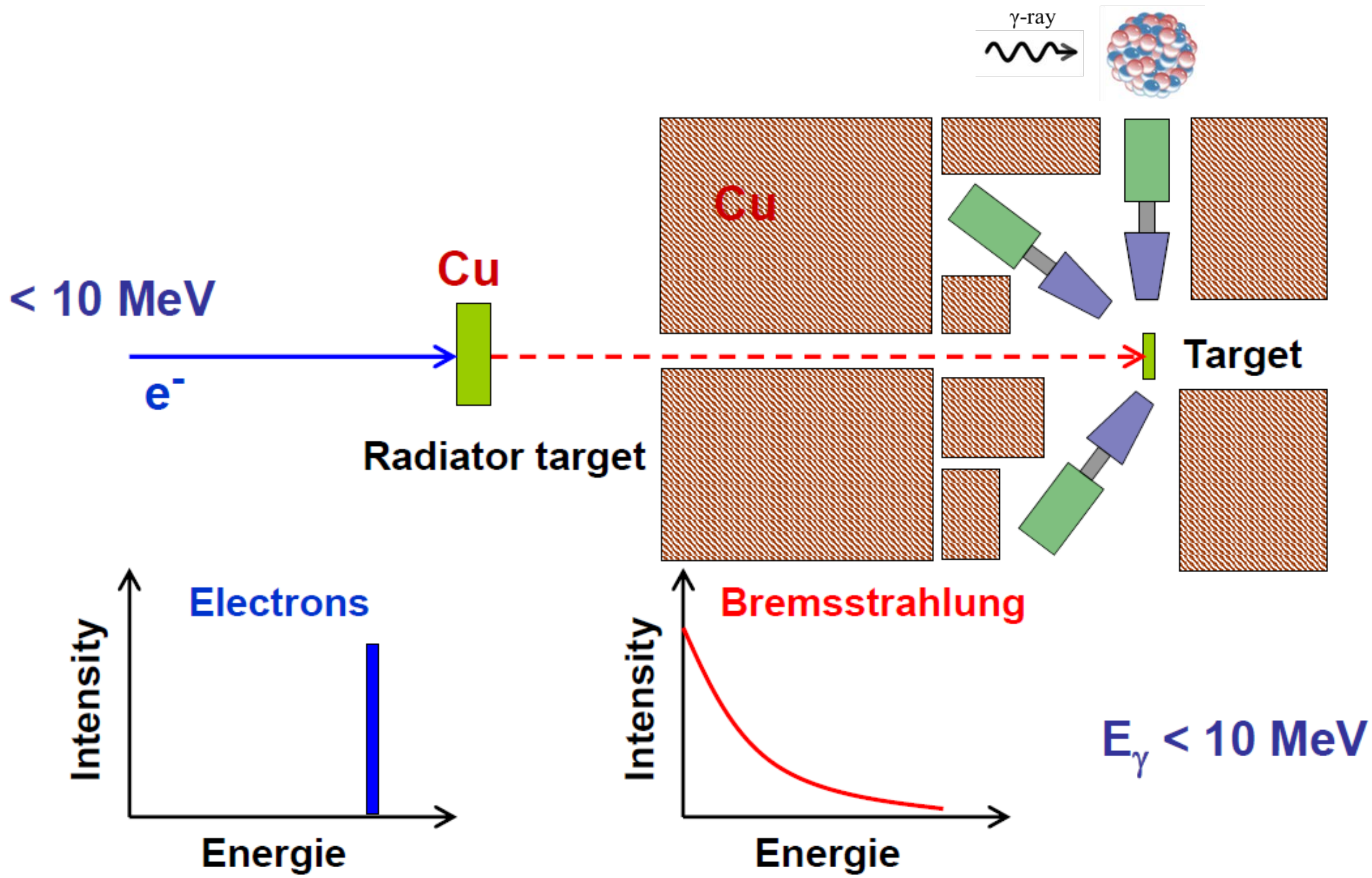

- “white“ photon spectrum
- wide energy region examined

Absorption processes

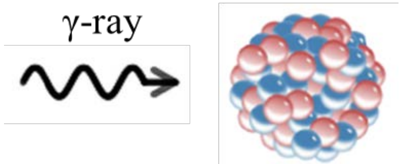

Absorption lines only a few eV wide!

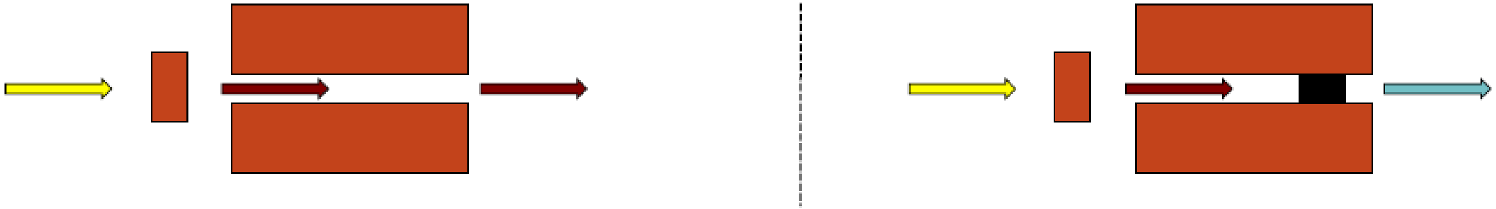

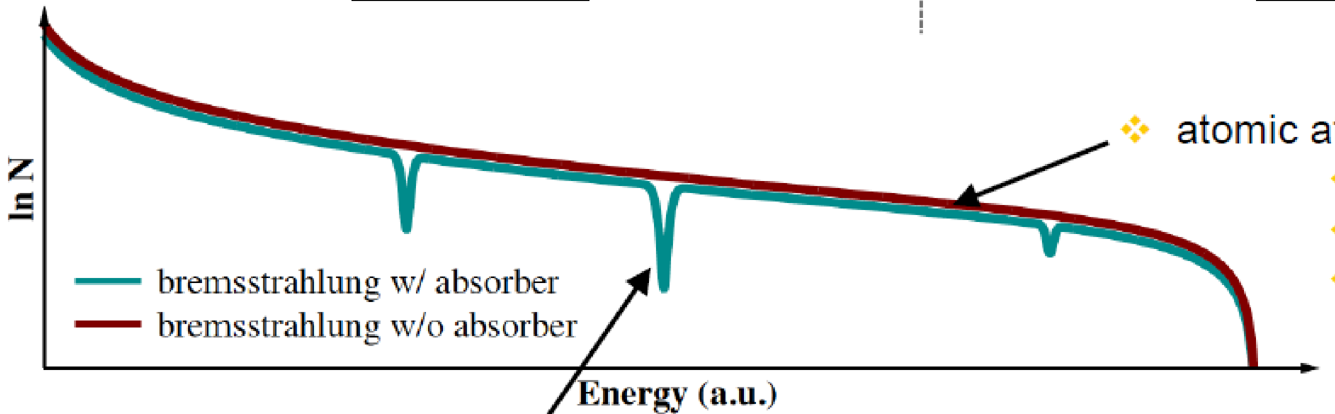

- atomic attenuation
  - several processes
  - contributes at each energy
  - independent of Γ_0

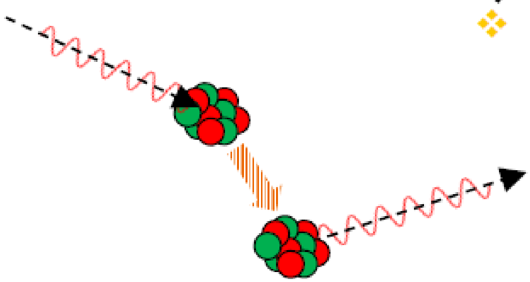

- resonant absorption
  - only at resonance energies
  - depends on Γ_0

$$\sigma_a \propto \Gamma_0 \cdot e^{-\left(\frac{E-E_r}{\Delta}\right)^2}$$

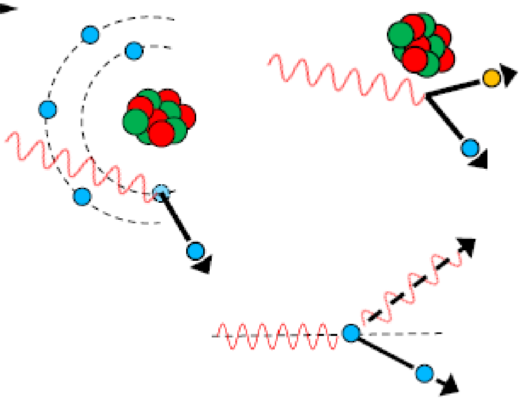

Principle of measurement and self absorption

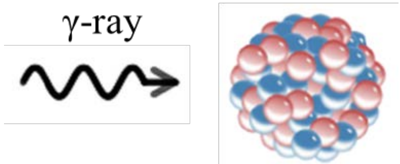

Use scatterer made of absorber material as „high-resolution detector“.

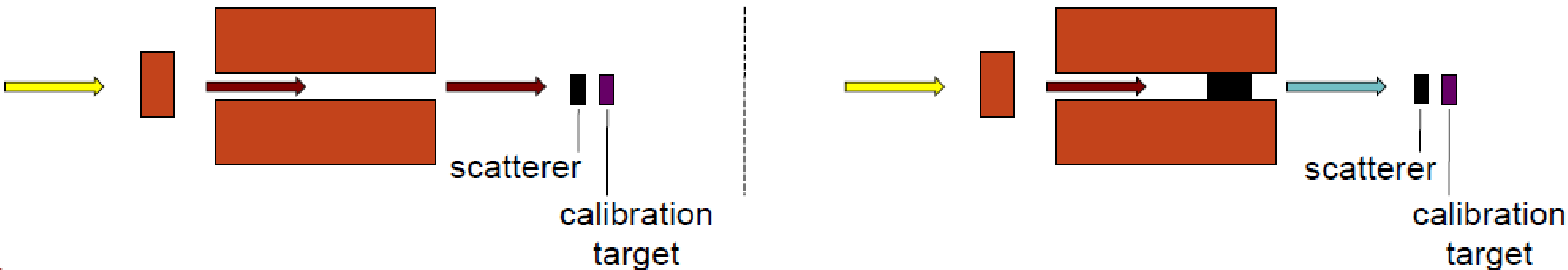

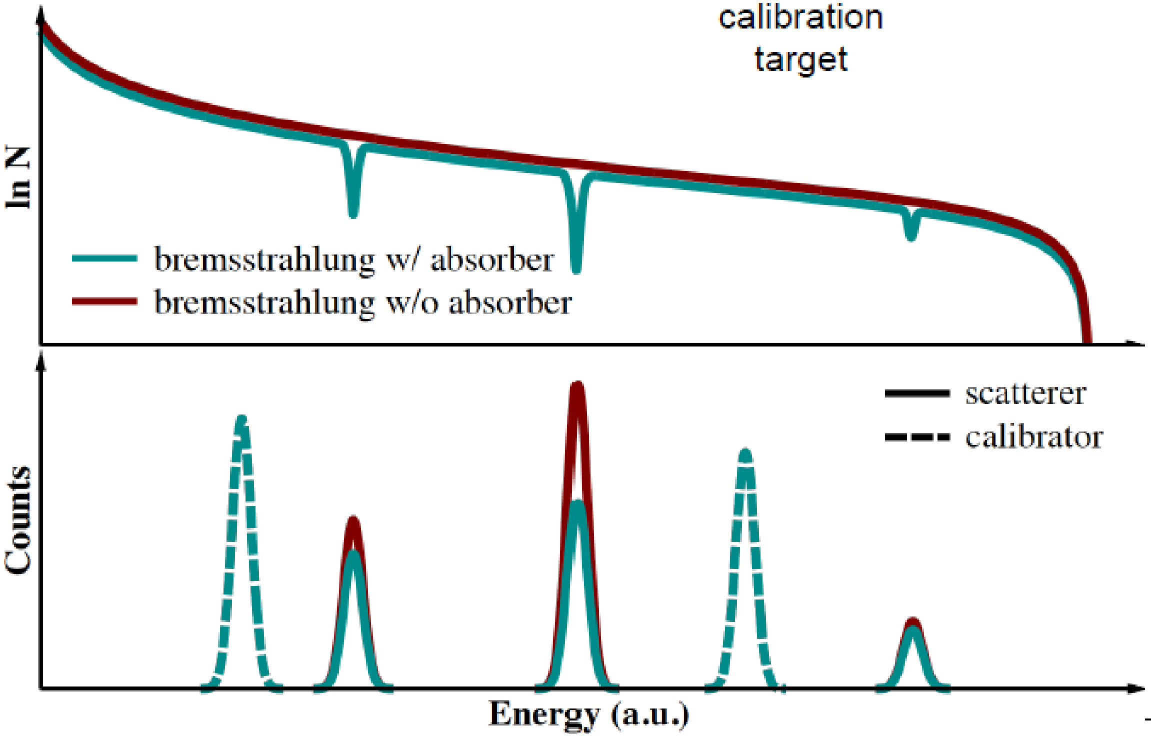

Self Absorption:
Decrease of Scattered Photons because of Resonant Absorption

$$R(\Gamma_0) = \frac{N_{\mathrm{woA}} - f \cdot N_{\mathrm{wA}}}{N_{\mathrm{woA}}}$$

$$f = \frac{N^{\mathrm{std}}_{\mathrm{woA}}}{N^{\mathrm{std}}_{\mathrm{wA}}}$$

First γγ-coincidences in a γ-beam

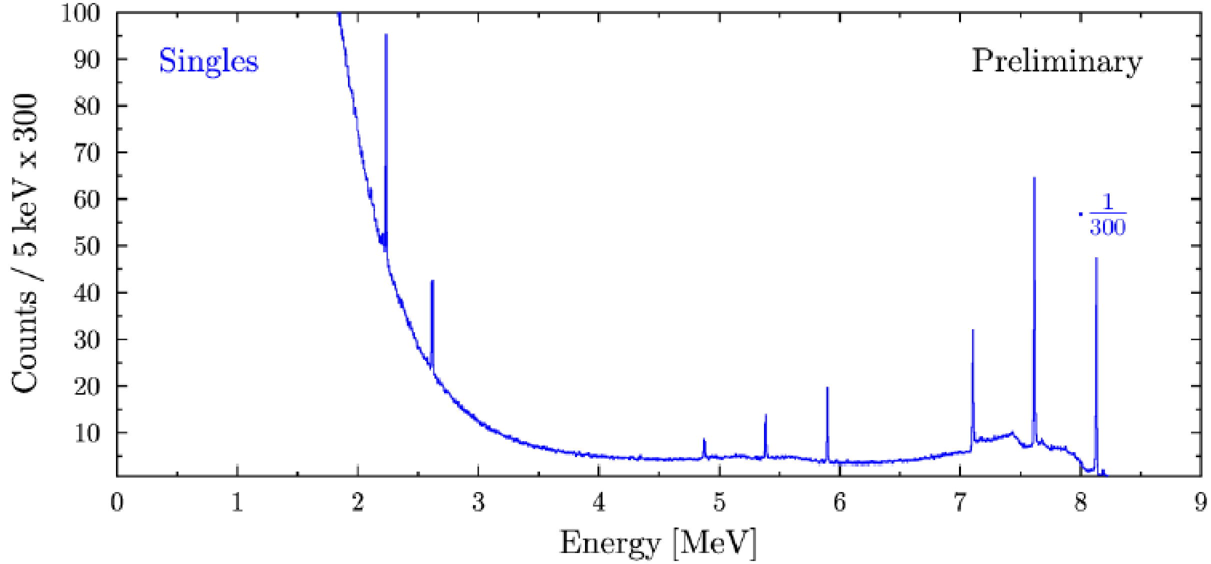

B. Löher et al., Nucl. Instruments Methods Phys. Res. Sect. A **723**, 136–142 (2013).

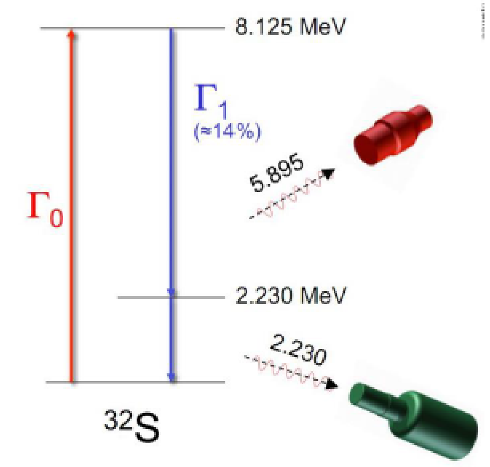

First γγ-coincidences in a γ-beam

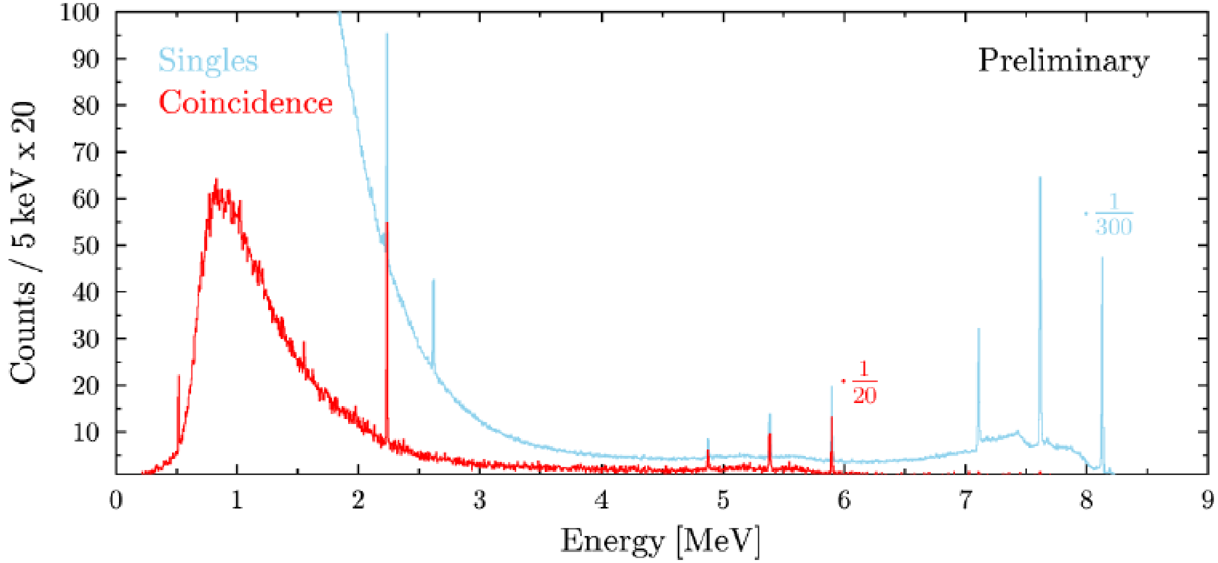

B. Löher et al., Nucl. Instruments Methods Phys. Res. Sect. A **723**, 136–142 (2013).

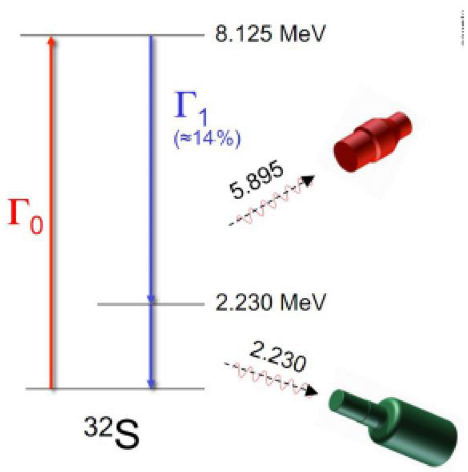

First γγ-coincidences in a γ-beam

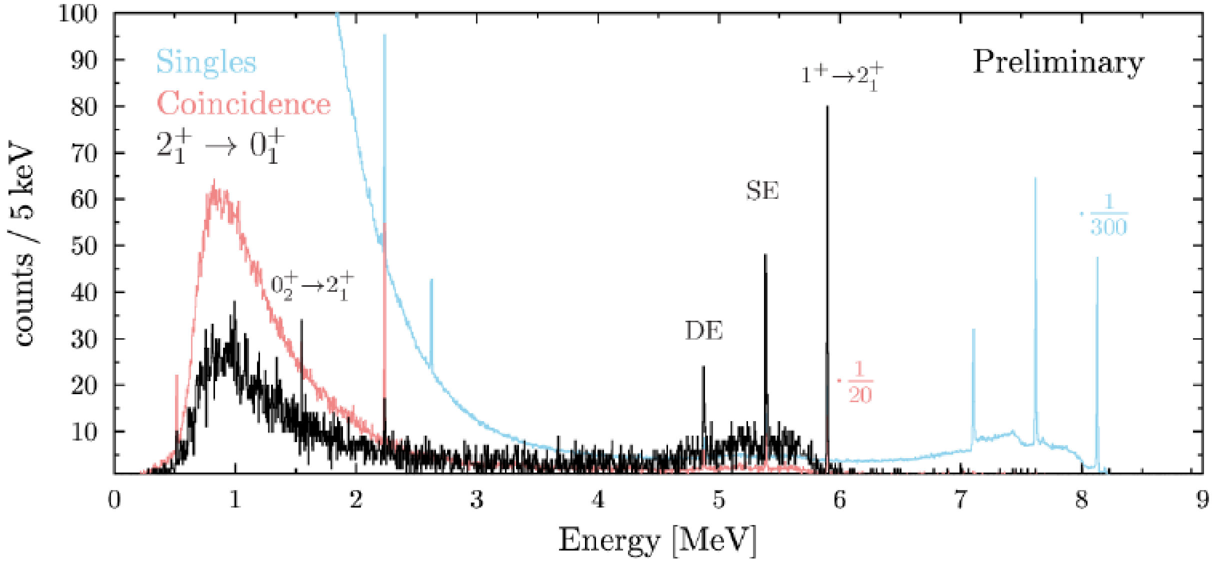

B. Löher et al., Nucl. Instruments Methods Phys. Res. Sect. A **723**, 136–142 (2013).

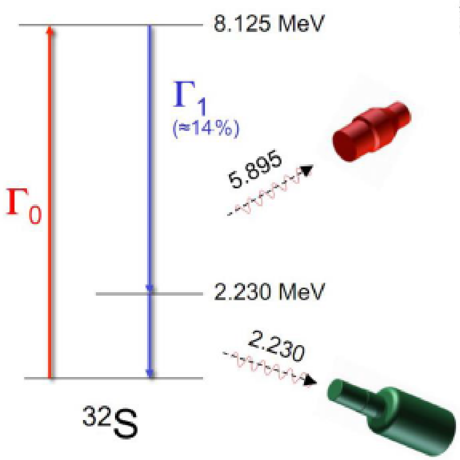

What is synchrotron radiation?

Electromagnetic radiation is emitted by charged particles when accelerated

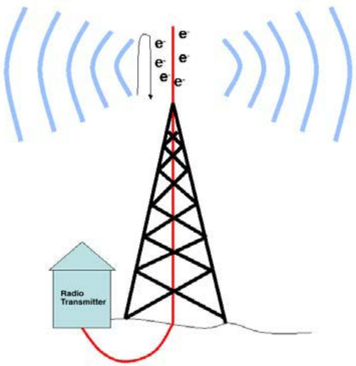

EM radiated from an antenna:
time-varying current runs up and down the antenna, and in the process emits radio waves

At the heart of the Crab nebula is a rapidly-spinning neutron star, a pulsar, and it powers the strongly polarized bluish ‘synchrotron’ nebula.

The electromagnetic radiation emitted when the charged particles are accelerated radially ($v \perp a$) is called synchrotron radiation.
It is produced in the synchrotron radiation source using bending magnets, undulators and wigglers

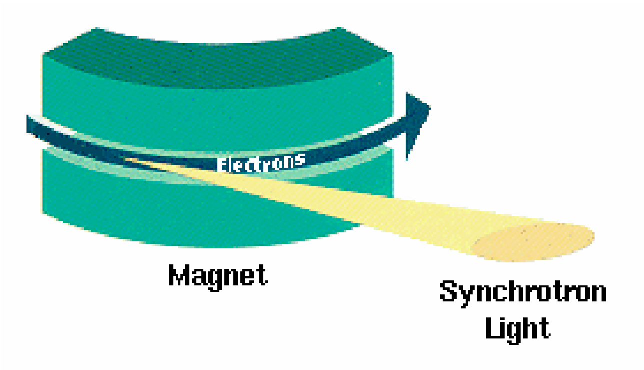

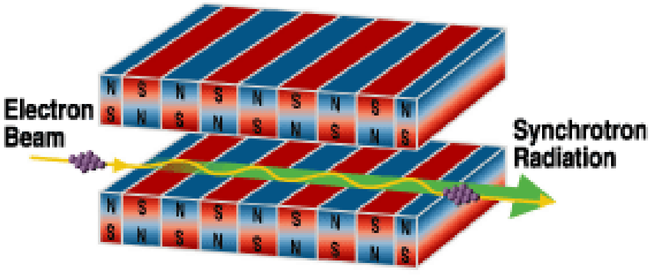

Properties of Synchrotron Radiation: Radiation Spectrum

The Electromagnetic Spectrum

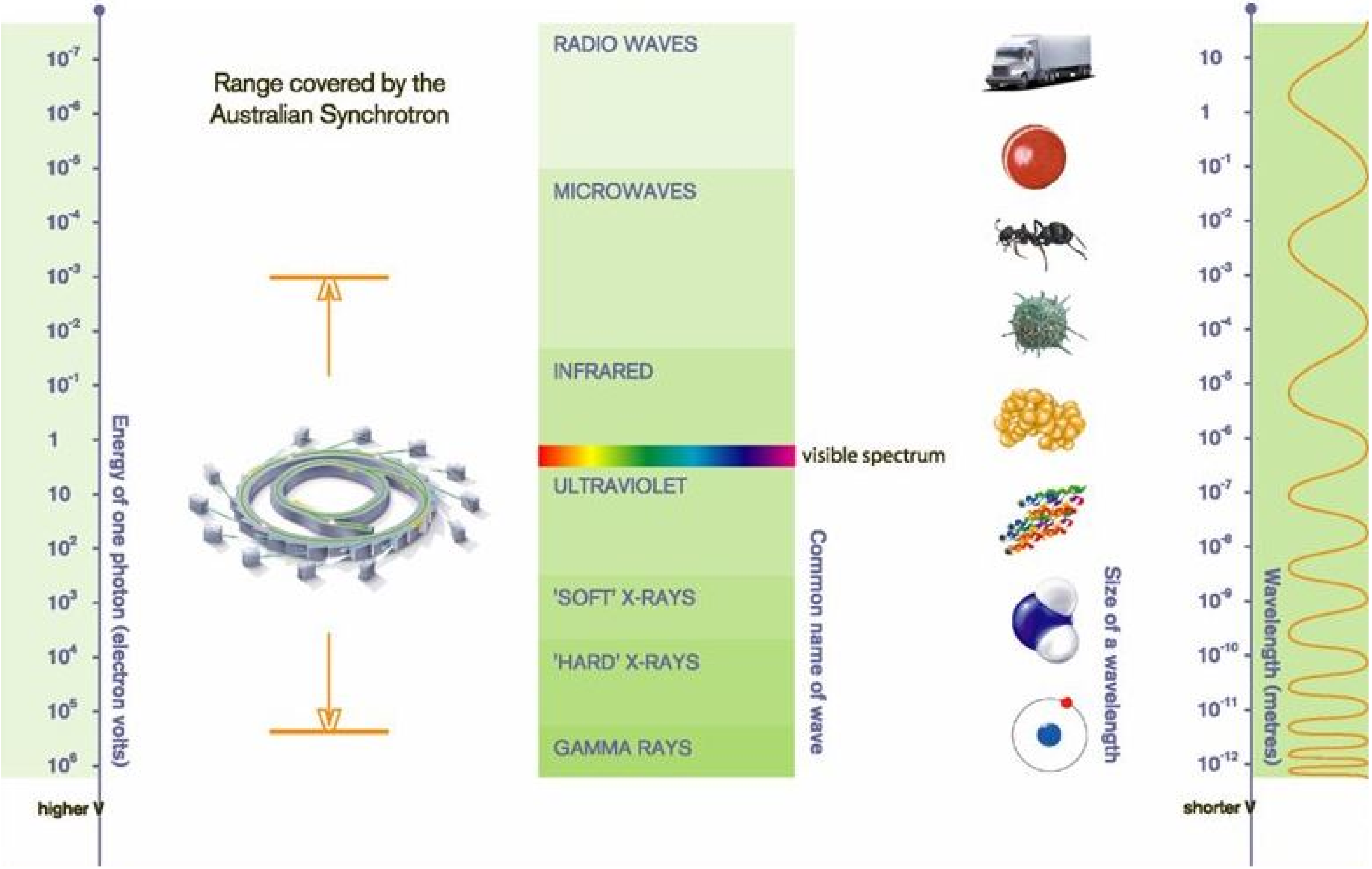

Discovery of X-rays ~100 years ago

- X-ray were discovered (accidentally) in 1895 by Wilhelm Konrad Roentgen.
- Roentgen won the first Nobel Prize in 1901 “for the discovery with which his name is linked for all time: the … so-called Roentgen rays, as he himself called them, X-rays …”

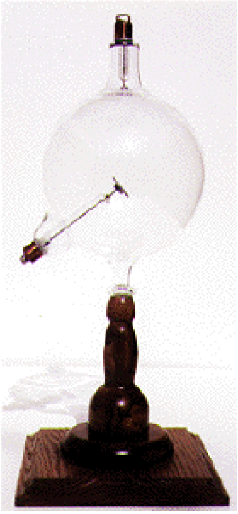

first commercial X-ray tube

Synchrotron Radiation

Lorentz Force: $\vec{F} = q \cdot (\vec{E} + \vec{v} \times \vec{B})$

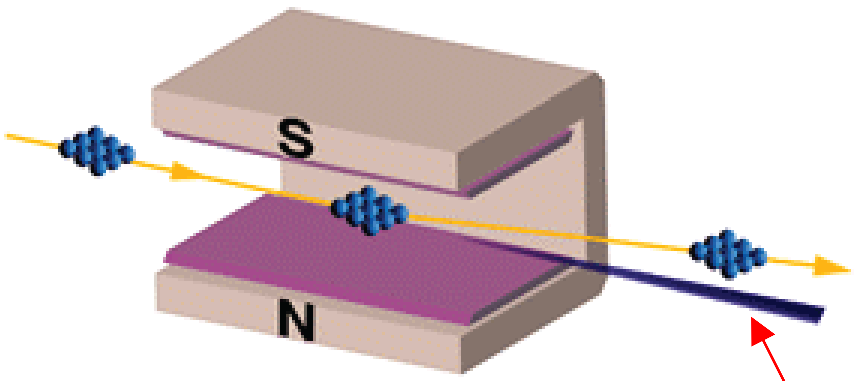

Synchrotron Radiation

Electromagnetic radiation produced by relativistic charged particles accelerated in circular orbits.

Discovery of Synchrotron Radiation ~50 years ago

Synchrotron radiation was first observed (accidentally) from a 70 MeV synchrotron in 1947

On April 24, 1947 Langmuir and I [Herbert Pollack] were running the machine and as usual were trying to push the electron gun and its associated pulse transformer to the limit. Some intermittent sparking had occurred and we asked the technician to observe with a mirror around the protective concrete wall. He immediately signaled to turn off the synchrotron as "he saw an arc in the tube". The vacuum was still excellent, so Langmuir and I came to the end of the wall and observed. At first we thought it might be due to Cherenkow radiation, but it soon became clear that we were seeing Ivanenko and Pomeranchuk [i.e. synchrotron] radiation.

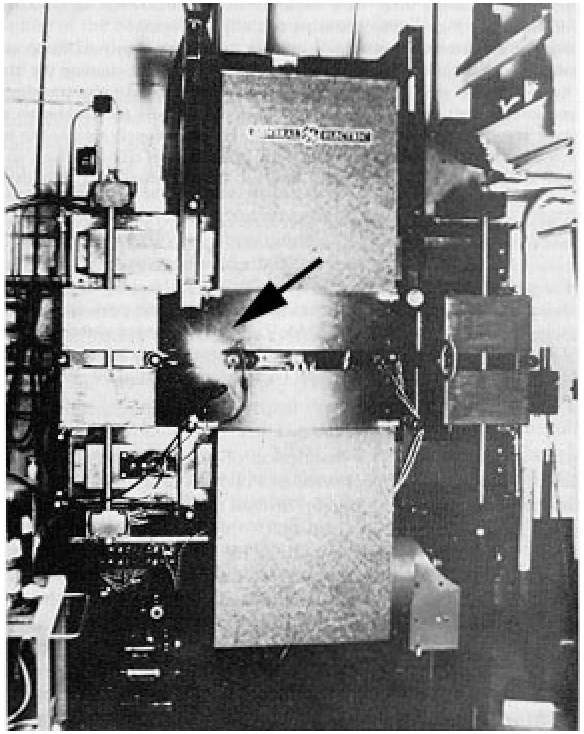

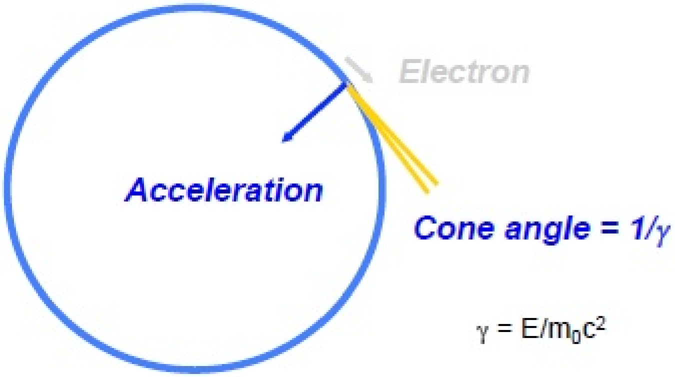

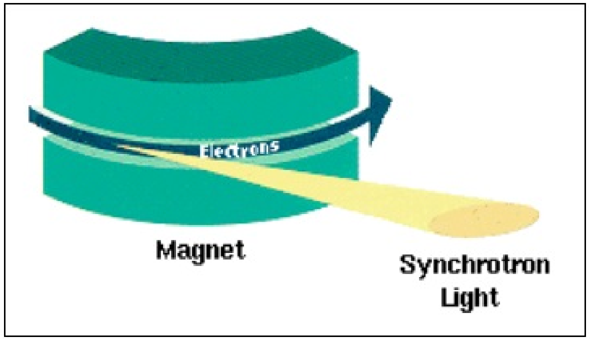

Charge at rest: Coulomb field, no radiation

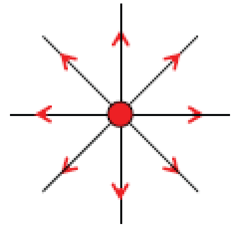

Uniformly moving charge, no radiation
(Cherenkov radiation)

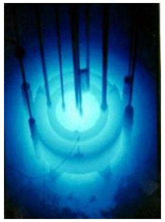

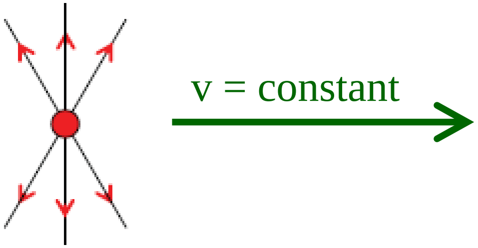

Accelerating charge

- ➢ $v \parallel a \rightarrow$ ***Bremsstrahlung***, antennas

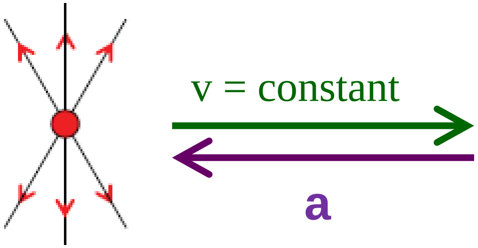

- ➢ $v \perp a \rightarrow$ ***Synchrotron radiation***

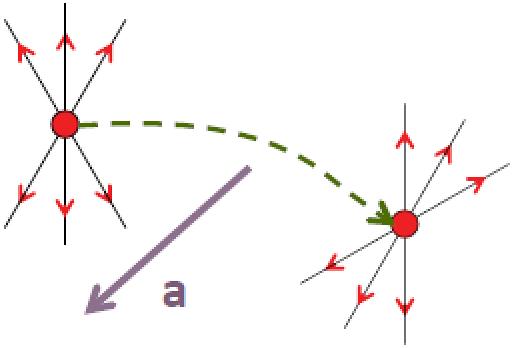

Properties of Synchrotron Radiation: Angular Distribution

- Radiation becomes more focused at higher energies

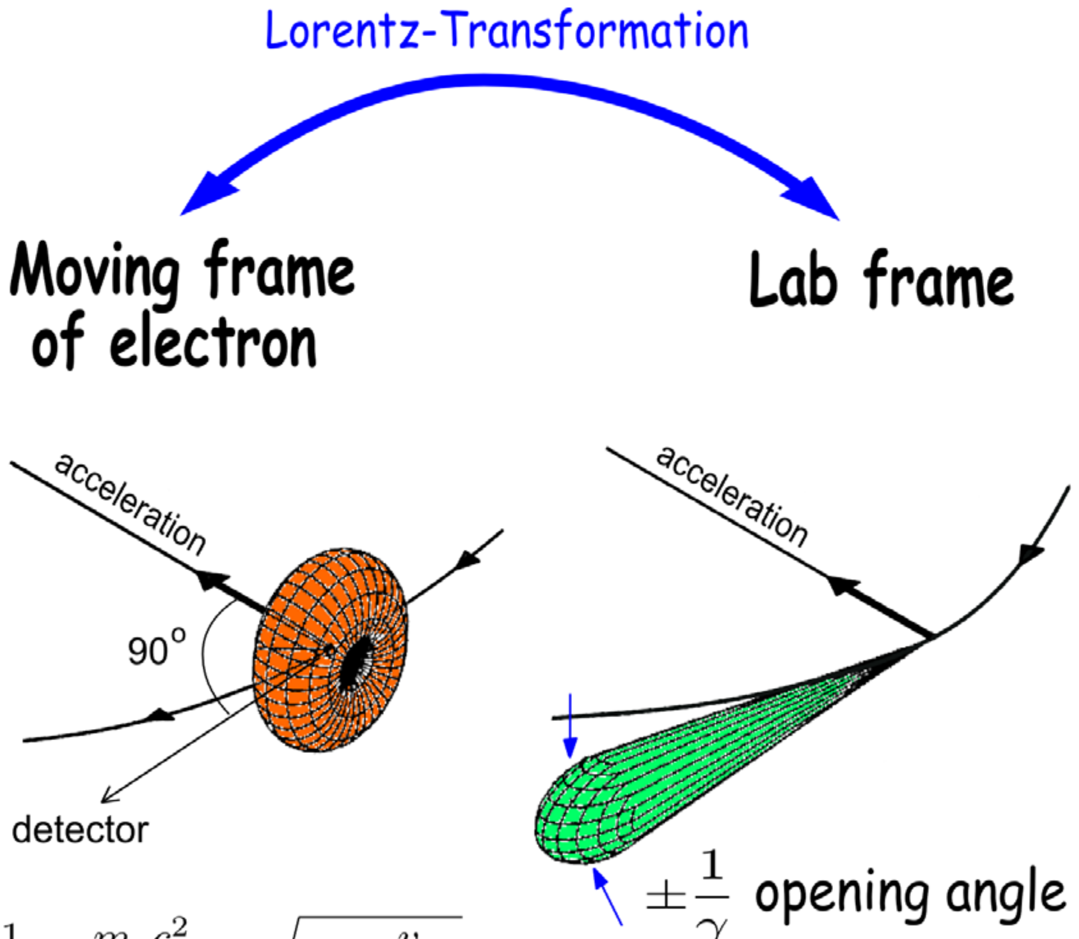

$$\frac{1}{\gamma} = \frac{m_o c^2}{E} = \sqrt{1 - (\frac{v}{c})^2}$$

Synchrotron radiation from relativistic electrons

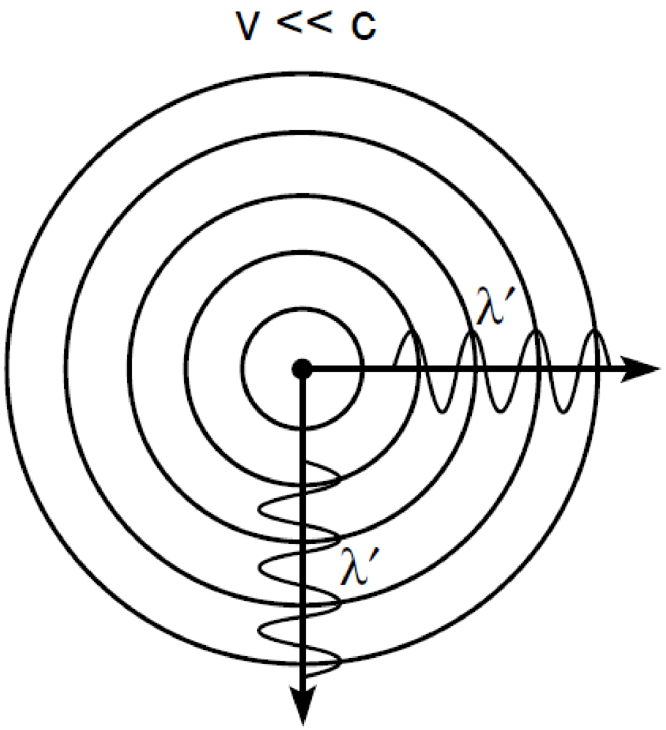

$$\lambda \cong \lambda' \cdot (1 - \beta \cdot cos\theta)$$

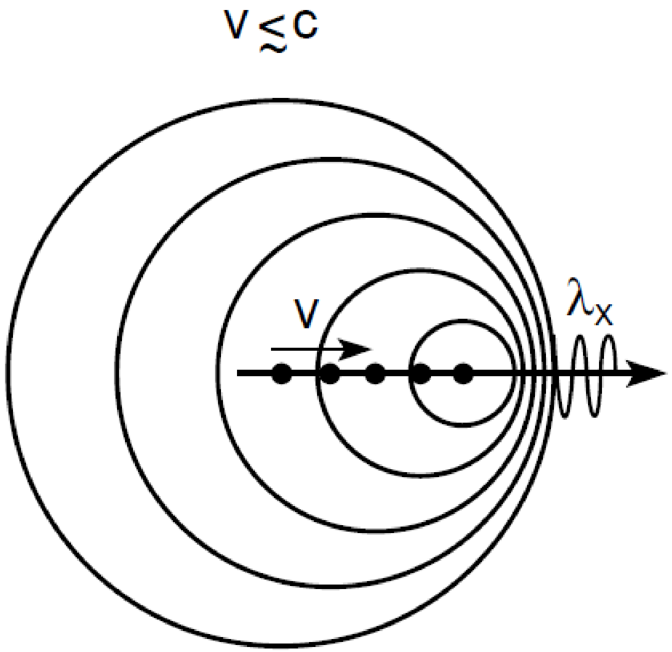

angle dependent Doppler shift

$$\lambda = \lambda' \cdot \frac{1 - \beta \cdot cos\theta}{\sqrt{1 - \beta^2}}$$

$$E_\gamma = E_{\gamma 0} \cdot \frac{\sqrt{1 - \beta^2}}{1 - \beta \cdot cos\theta}$$

Synchrotron radiation from relativistic electrons

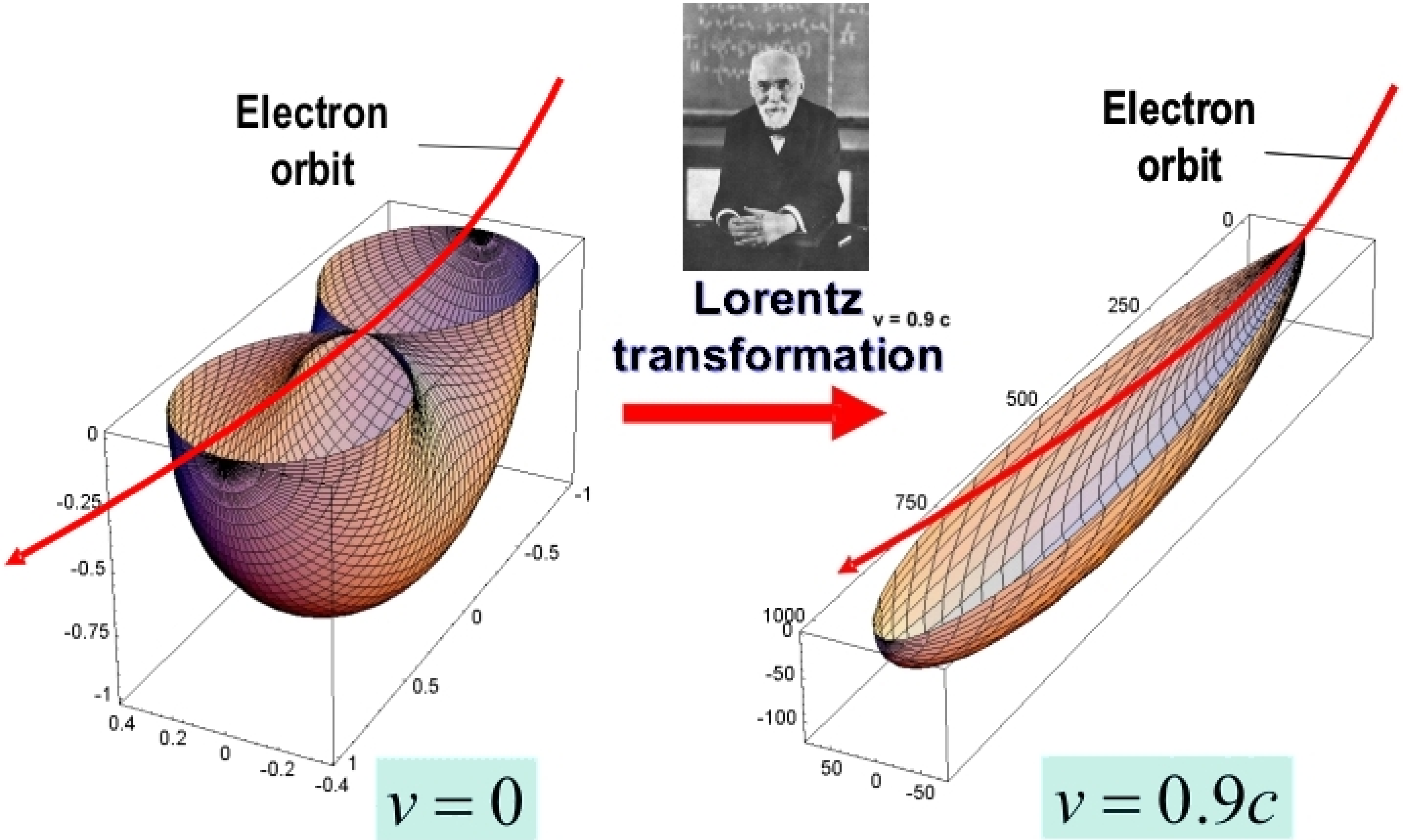

$$\boxed{\frac{d\Omega_{rest}}{d\Omega_{lab}} = \left(\frac{E_\gamma}{E_{\gamma 0}}\right)^2}$$

$$\frac{E_\gamma}{E_{\gamma 0}} = \frac{\sqrt{1-\beta^2}}{1-\beta \cdot cos\theta}$$

Radiation Patterns when *v* approaches *c*

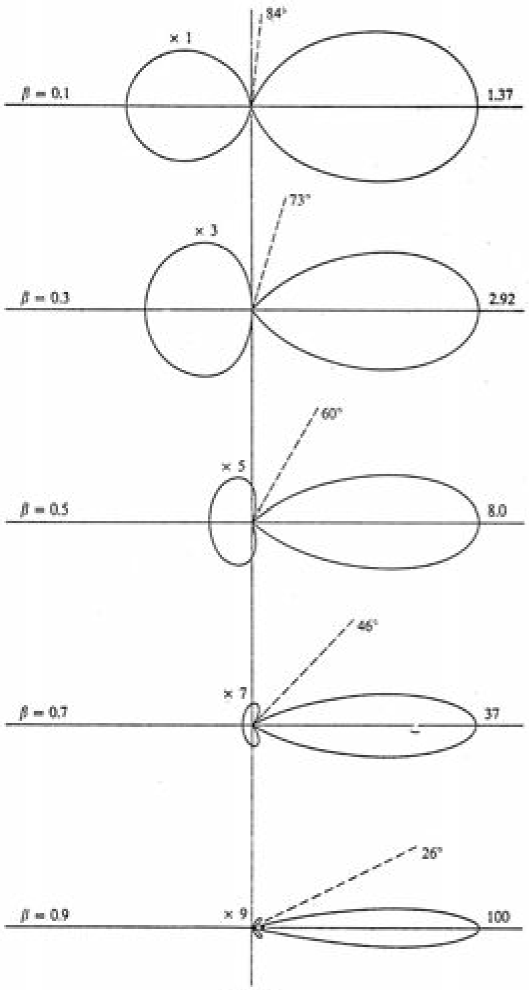

Fig. 7-7

As $\boldsymbol{\beta}$ approaches **1**:

a. The shape of the radiation pattern is changing; it is more forward peaked

b. The size of the radiation pattern is changing; it is getting bigger

So at $\boldsymbol{\beta \approx 1}$, the node at $\boldsymbol{\theta' = 90^0}$ (in the frame of the radiating particle, rest frame) transforms to:

$$\boxed{tan\theta_{lab} = \frac{sin\theta'}{\gamma \cdot (cos\theta' + \beta)} = \frac{1}{\gamma \cdot \beta} \approx \frac{1}{\gamma}}$$

In fact, the ***opening angle*** in both the horizontal and vertical directions, is given approximately by:

$$\boxed{\theta = \frac{1}{\gamma}}$$

Consider a charged particle in homogeneous field B

❖ The acceleration in ***B*** is given by

$$\dot{\vec{\beta}}_{\perp} = \frac{\beta^2 c}{\rho} \qquad m\dot{v} = \frac{mv^2}{\rho}$$

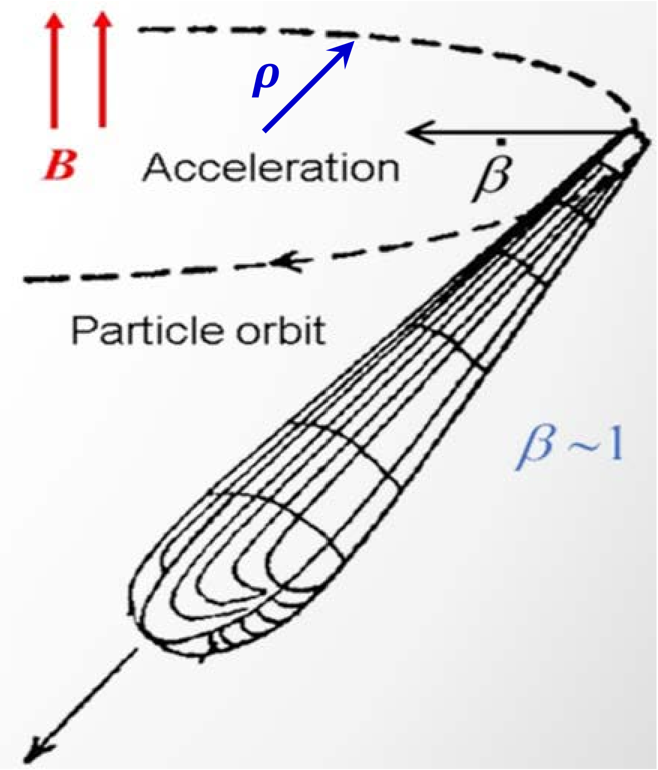

where the bending radius of charged particle, ρ, at energy E_e is

$$\frac{1}{\rho[m]} = \frac{e \cdot B \cdot c}{\beta \cdot E_e} = 0.2998 \frac{B[T]}{\beta \cdot E_e[GeV]}$$

Larmor radius $\rho = \frac{mv}{e \cdot B} = \frac{mc^2 \cdot v}{e \cdot B \cdot c^2} = \frac{E_e \cdot \beta}{e \cdot \beta \cdot c}$

Then the instantaneous radiation power becomes

$$P = \frac{2 \cdot c \cdot r_e \cdot m_e c^2}{3} \cdot \frac{\beta^4 \cdot \gamma^4}{\rho^2} = \frac{c \cdot C_\gamma}{2\pi} \cdot \frac{E_e^4}{\rho^2}$$

$$C_\gamma \equiv \frac{4\pi}{3} \cdot \frac{r_e}{(m_e c^2)^3} = 8.85 \cdot 10^{-5} \left[\frac{m}{GeV^3}\right]$$

classical electron radius $r_e = \frac{e}{4\pi \cdot \varepsilon_0 \cdot m_e c^2}$

Synchrotron Radiation Power and Energy Loss for Electrons

- Instantaneous Synchrotron Radiation Power for a single electron

$$P_\gamma[GeV/s] = \frac{c \cdot C_\gamma}{2\pi} \cdot \frac{E^4[GeV^4]}{\rho^2[m^2]} \qquad \text{with} \qquad C_\gamma = 8.8575 \cdot 10^{-5} \frac{m}{GeV^3}$$

- Energy loss per turn for a single particle in an isomagnetic lattice with bending radius ρ is given by integrating P_γ over the lattice

$$\Delta E[GeV] = C_\gamma \cdot \frac{E^4[GeV^4]}{\rho[m]}$$

- The average Radiated Power for an entire beam is $(P = {}^{I}/_{e} \cdot \Delta E)$

$$P_\gamma[MW] = 8.8575 \cdot 10^{-2} \cdot \frac{E^4[GeV^4]}{\rho[m]} \cdot I[A]$$

- Radiated Power varies as the inverse fourth power of particle mass. Comparing radiated power from a proton vs. an electron, we have: $\frac{P_e}{P_p} = \left(\frac{m_p}{m_e}\right)^4 = 1836^4 = 1.1367 \cdot 10^{13}$

$$P_\gamma[MW] = 2.65 \cdot 10^{-2} \cdot E^3\,[GeV]^3 \cdot B\,[T] \cdot I\,[A]$$

❖ Total photon numbers

$$\dot{N}_{ph,Ie} = \frac{15\sqrt{3}\pi}{4} C_\psi I_e E_e$$

$$= 8.08\times 10^{20}\, I[\mathrm{A}] E_e[\mathrm{GeV}] \quad [\mathrm{photons/s}]$$

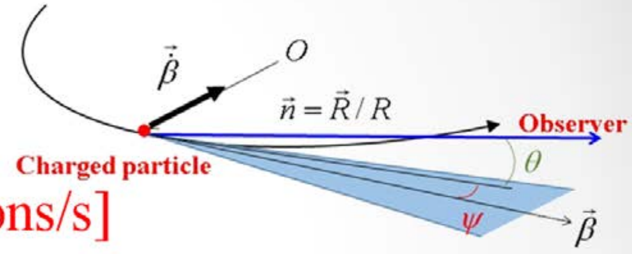

Some useful formulas for synchrotron radiation

$$\gamma = \frac{1}{\sqrt{1-\frac{v^2}{c^2}}} = \frac{1}{\sqrt{1-\beta^2}}; \quad \beta = \frac{v}{c}; \quad (1-\beta) \cong \frac{1}{2\gamma^2}$$

$$E_e = \gamma \cdot mc^2; \quad p = \gamma \cdot mv$$

$$\gamma = \frac{E_e}{mc^2} = 1957 \cdot E_e\,[GeV]$$

$$\hbar\omega \cdot \lambda = 1239.842\,[eV \cdot nm]$$

$$1\,Watt \Rightarrow 5.034 \cdot 10^{15} \cdot \lambda\,[nm] \cdot \frac{photons}{s}$$

$$Bending\ Magnet\colon\ E_c = \frac{3e \cdot \hbar \cdot B \cdot \gamma^2}{2m}; \quad E_c(keV) = 0.6650 E_e^2\,[GeV] \cdot B[T]$$

$$Undulator\colon\ \lambda = \frac{\lambda_u}{2\gamma^2} \cdot \left(1 + \frac{K^2}{2} + \gamma^2 \cdot \theta^2\right); \quad E(keV) = \frac{0.9496 \cdot E_e^2\,(GeV)}{\lambda_u(cm) \cdot \left(1 + \frac{K^2}{2} + \gamma^2 \cdot \theta^2\right)}$$

where $K \equiv \frac{e \cdot B_0 \cdot \lambda_u}{2\pi \cdot mc} = 0.9337 \cdot B_0(T) \cdot \lambda_u(cm)$

Accelerator Synchrotron Sources

- Synchrotron radiation is generated in normal accelerator bending magnets

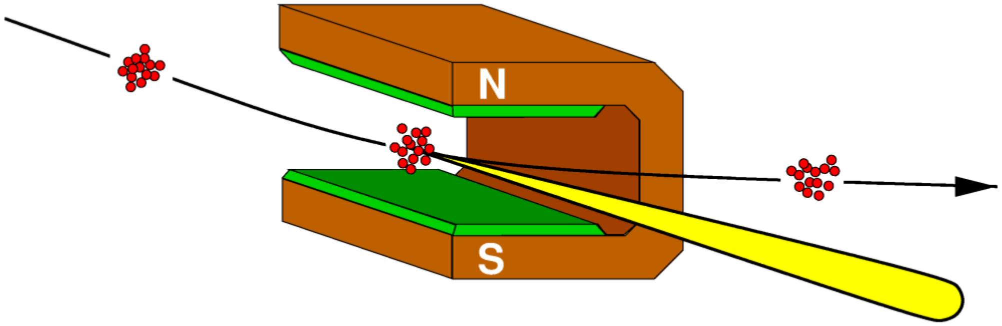

- There are also special magnets called wigglers and undulators which are designed for this purpose.

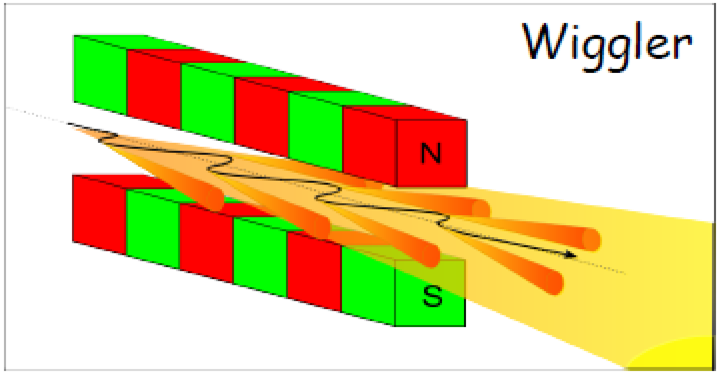

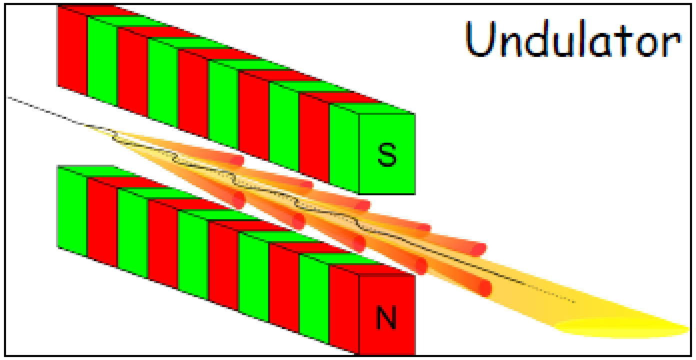

Layout of a synchrotron radiation source

Electrons are generated and accelerated in a ***LINAC***, further accelerated to the required energy in a ***booster*** and injected and stored in a ***storage ring***.
The circulating electrons emit an intense beam of synchrotron radiation which is sent down the beamlines.

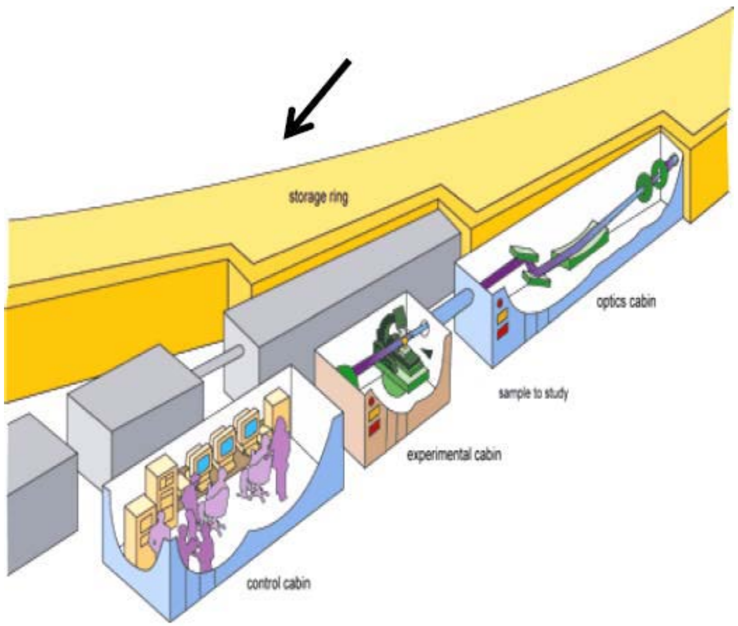

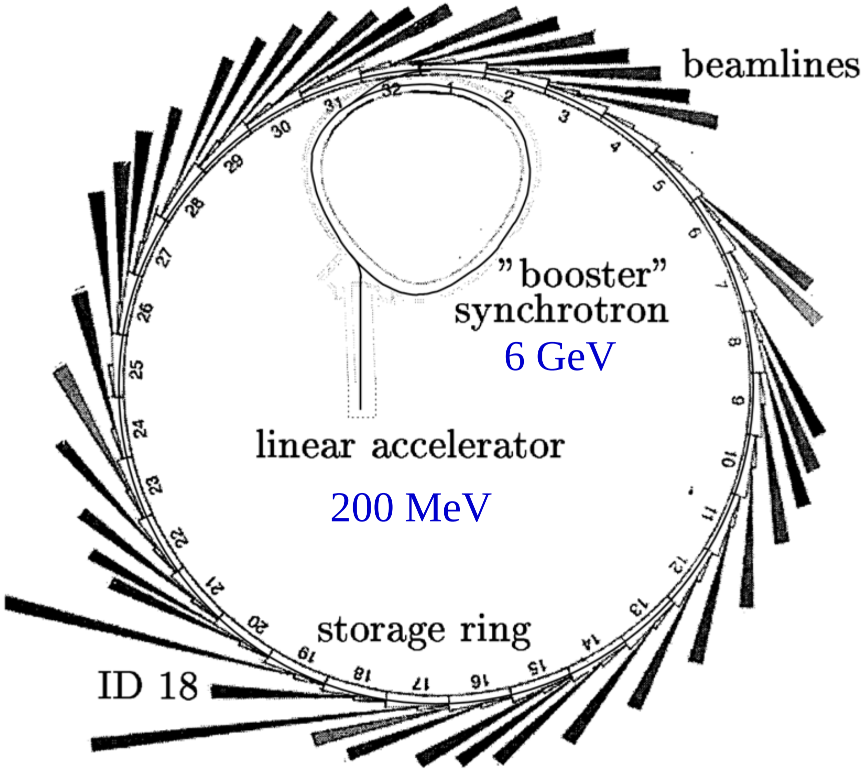

Synchrotron Light Sources

Synchrotron Radiation Spectrum

Bending Magnet Radiation covers a broad region of the spectrum, including the primary absorption edges of most elements.

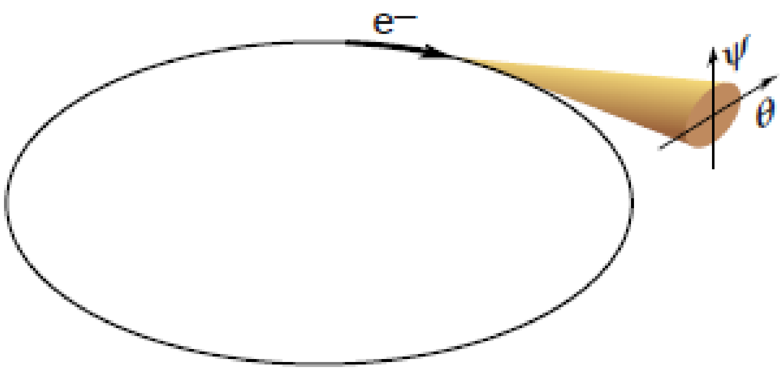

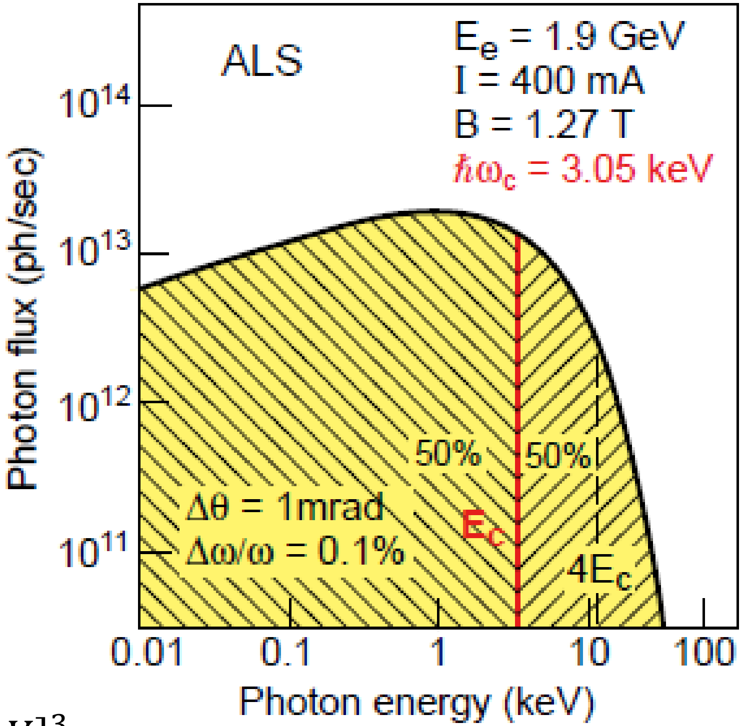

$$E_c = \hbar\omega_c = \frac{3e \cdot \hbar \cdot B \cdot \gamma^2}{2m}$$

$$E_c(keV) = 0.6650 \cdot E_e^2(GeV) \cdot B(T) \ = 2.218 \cdot \frac{E_e^3[GeV]^3}{\rho[m]}$$

$$\frac{d^2F_B}{d\theta \ \ d\omega/\omega} = 2.46 \cdot 10^{13} E_e(GeV) \cdot I(A) \cdot G_1(E/E_c) \cdot \frac{photons/s}{mrad \cdot (0.1\%BW)}$$

Advantages: cover broad spectral range
least expensive
most accessible

Disadvantages: limited coverage of hard X-rays
not as bright as undulator

Insertion Devices

Undulator: Electron beam is periodically deflected by a weak magnetic field. Particle emits radiation at wavelength of the periodic motion, divided by γ^2. So period of cm for magnets results in radiation in VUV to X-ray regime.

Wiggler: Electron beam is periodically deflected by strong bending magnets. Motion is no longer pure sinusoid and radiation spectrum is continuous up to a critical cut off photon energy ($\varepsilon_{crit} \sim B \cdot \gamma^2$). Spectrum is infrared to hard X-rays.

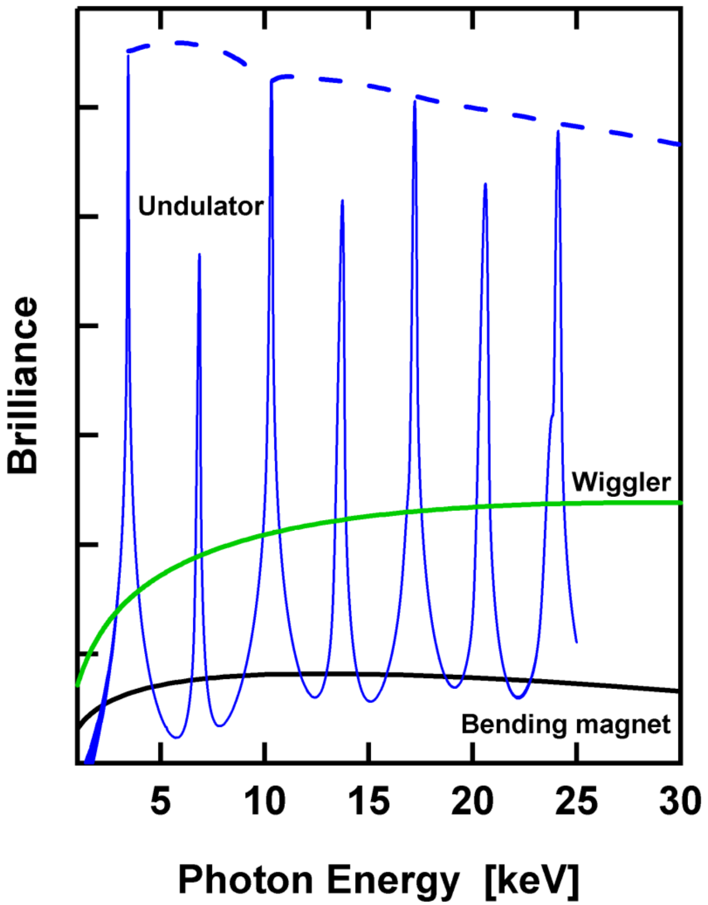

Three Forms of Synchrotron Radiation

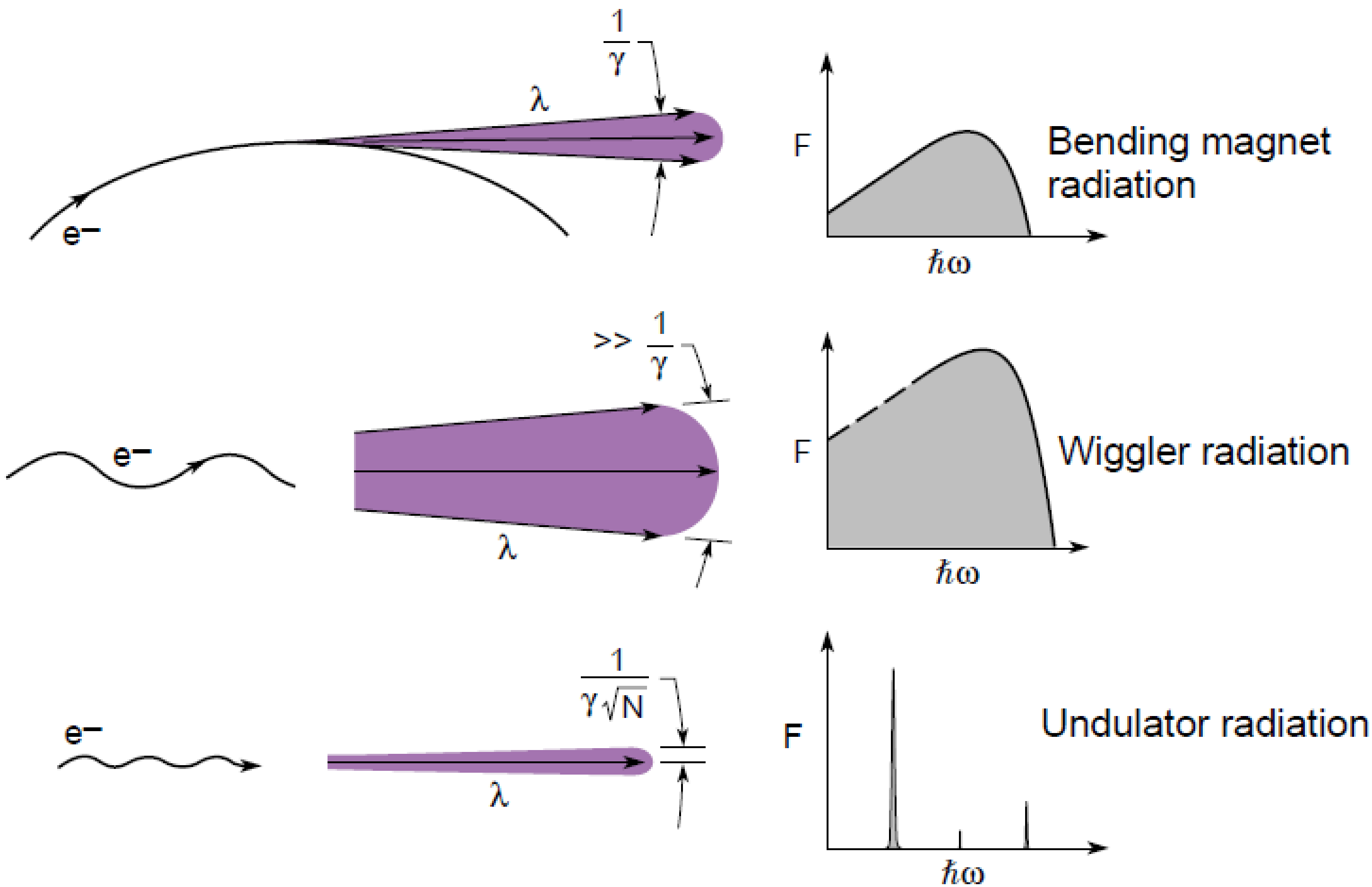

An Undulator up close

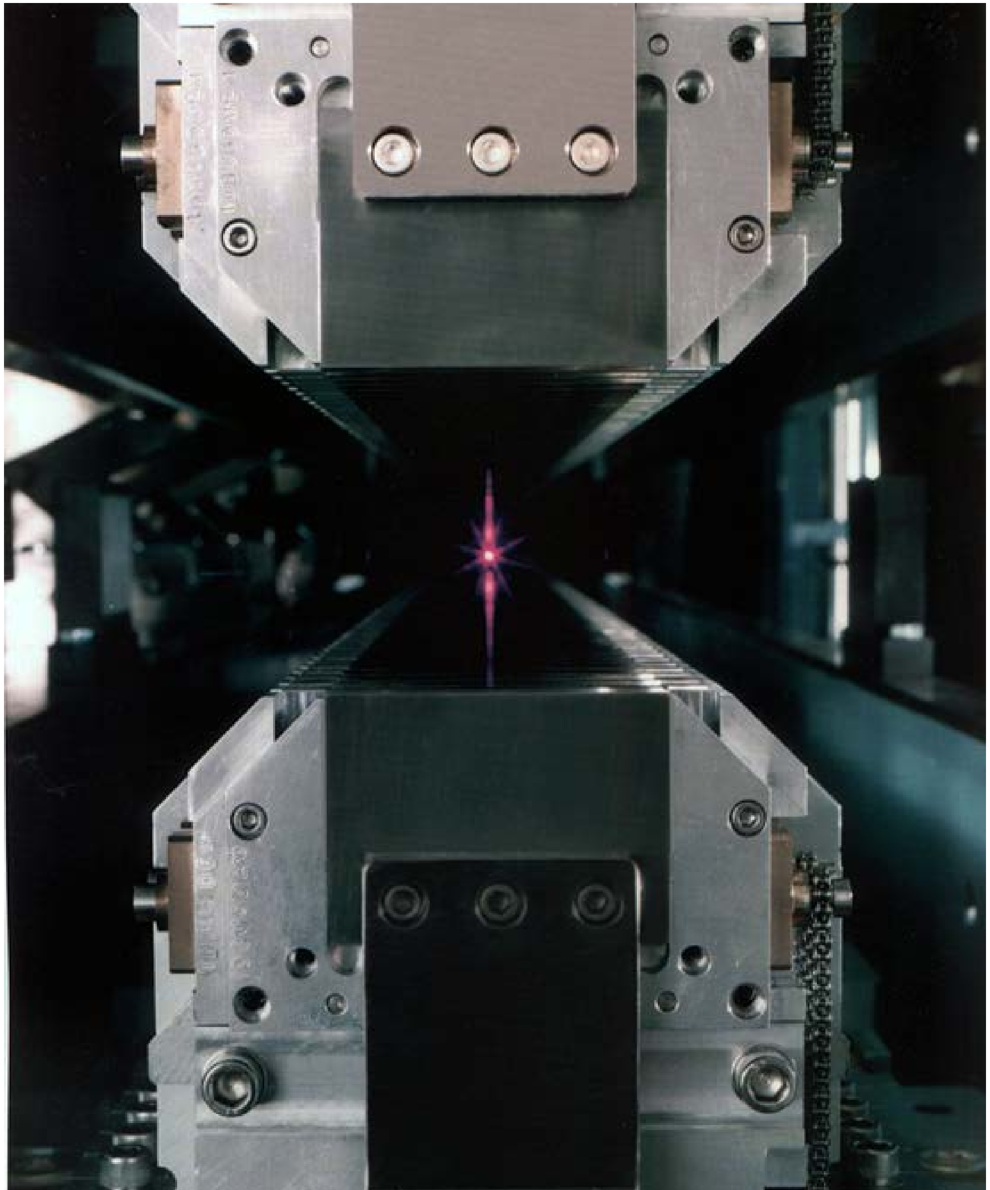

ALS U5 undulator, beamline 7.0, N = 89, $\lambda_u = 50\ mm$

Undulator Radiation

Laboratory Frame of Reference

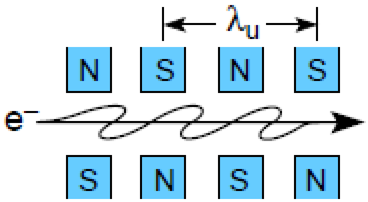

$E = \gamma mc^2$

$$\gamma = \frac{1}{\sqrt{1 - \frac{v^2}{c^2}}}$$

N = # periods

Frame of Moving e⁻

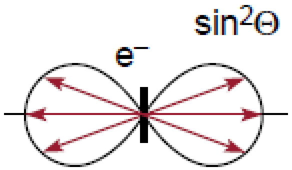

e^- radiates at the Lorentz contracted wavelength:

$$\lambda' = \frac{\lambda_u}{\gamma}$$

Bandwidth:

$$\frac{\lambda'}{\Delta\lambda'} \simeq N$$

Frame of Observer

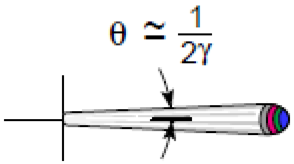

Doppler shortened wavelength on axis:

$$\lambda = \lambda'\gamma(1 - \beta\cos\theta)$$

$$\lambda = \frac{\lambda_u}{2\gamma^2}(1 + \gamma^2\theta^2)$$

Accounting for transverse motion due to the periodic magnetic field:

$$\boxed{\lambda = \frac{\lambda_u}{2\gamma^2}\left(1 + \frac{K^2}{2} + \gamma^2\theta^2\right)}$$

where $K = eB_0\lambda_u/2\pi mc$

Following Monochromator

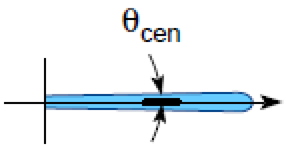

For $\frac{\Delta\lambda}{\lambda} \simeq \frac{1}{N}$

$$\theta_{cen} \simeq \frac{1}{\gamma\sqrt{N}}$$

typically

$$\theta_{cen} \simeq 40 \text{ rad}$$

How to characterize the properties of a synchrotron radiation source?

$$Total\ flux \equiv \frac{Photons}{s}$$

$$Spectral\ flux \equiv \frac{Photons/s}{0.1\%\ bandwidth}$$

$$Brightness \equiv \frac{Photons/s}{mrad^2 \cdot 0.1\%\ bandwidth}$$

$$Brilliance \equiv \frac{Photons/s}{mrad^2 \cdot mm^2 \cdot 0.1\%\ bandwidth}$$

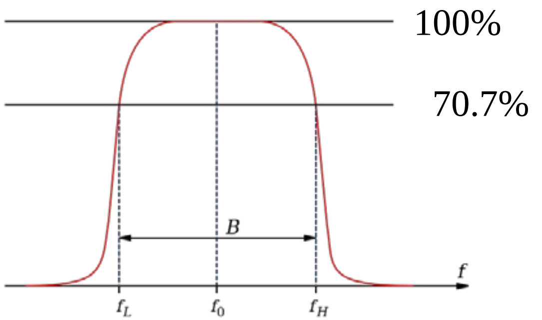

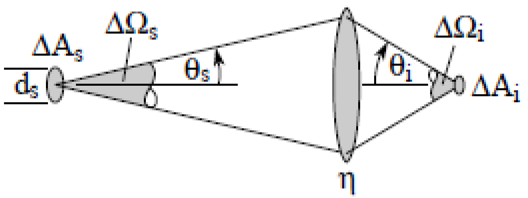

Brilliance is the figure of merit for the design of a new synchrotron source

Brilliance

Brilliance takes into account:

1. Number of photons produced per second
2. The angular divergence of the photons, or how fast the beam spreads out
3. The cross-section area of the beam
4. the photons falling within a bandwidth of 0.1% of the central wavelength or frequency

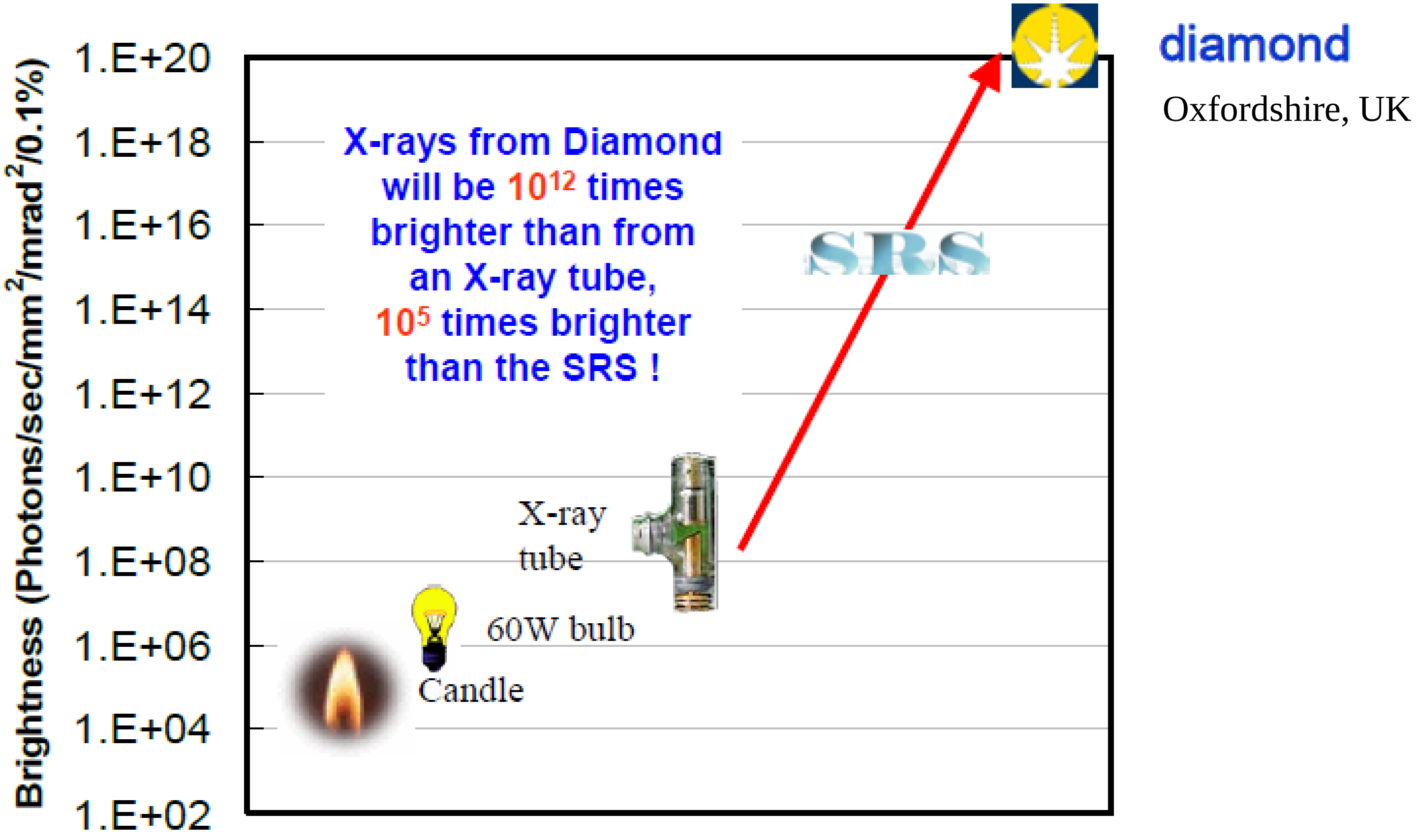

SRS = Synchrotron Radiation Source

Layout of a synchrotron radiation source

Electrons are generated and accelerated in a ***LINAC***, further accelerated to the required energy in a ***booster*** and injected and stored in a ***storage ring***.
The circulating electrons emit an intense beam of synchrotron radiation which is sent down the beamlines.

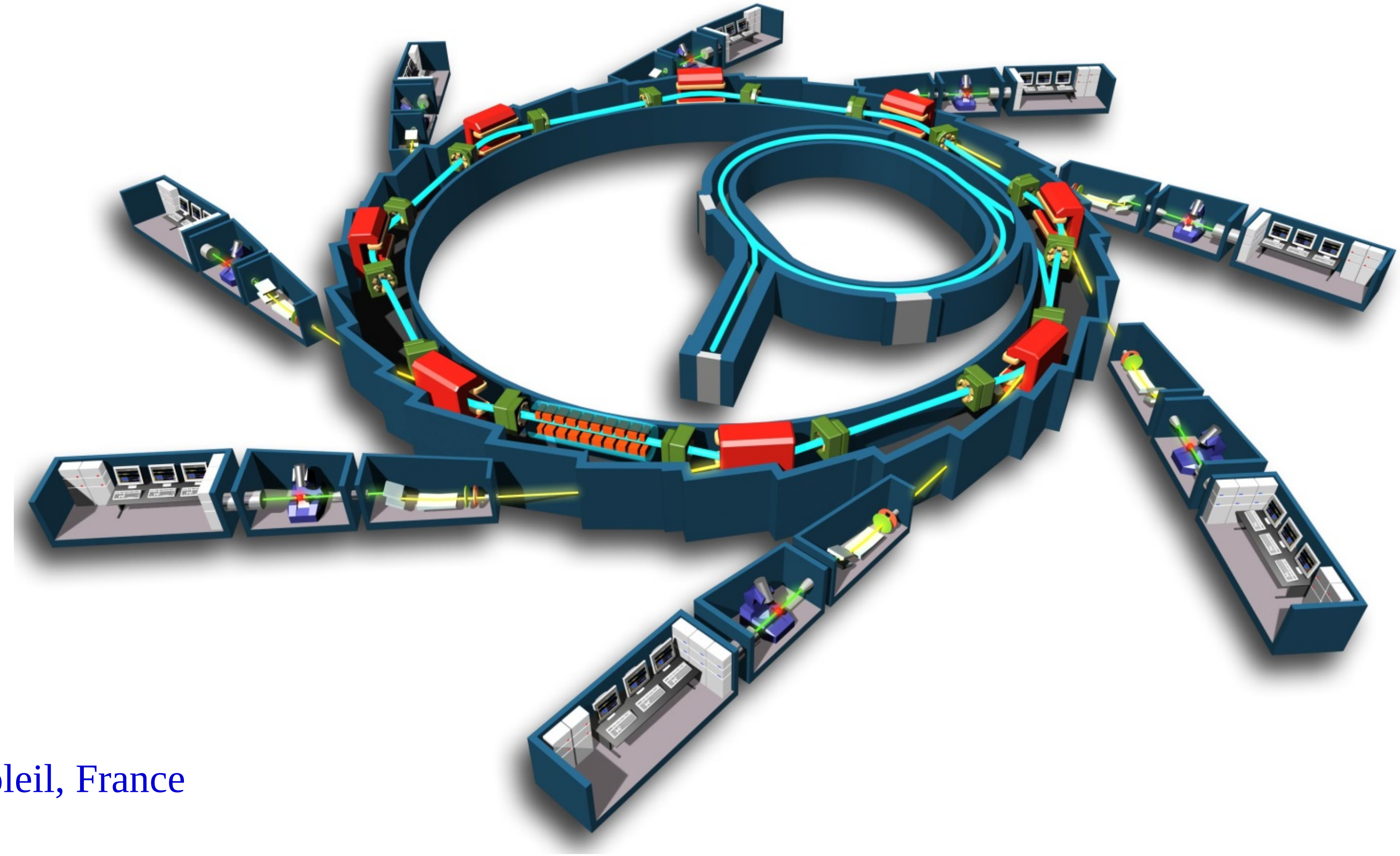

Soleil, France

Applications

Medicine, Biology, Chemistry, Material Science, Environmental Science and more

Biology

Reconstruction of the 3D structure of a nucleosome with a resolution of 0.2 nm

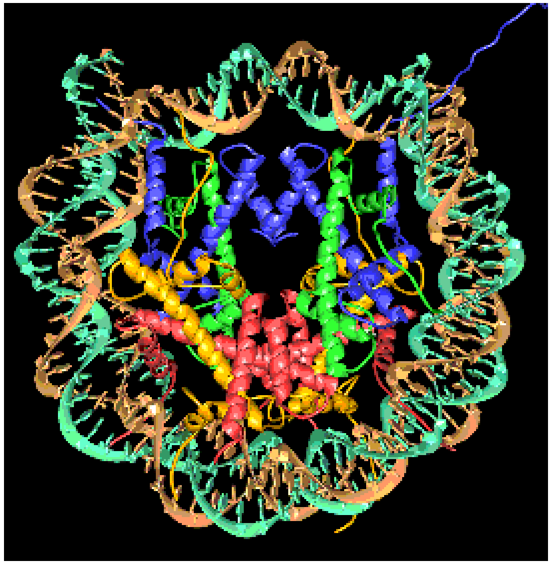

The collection of precise information on the molecular structure of chromosomes and their components can improve the knowledge of how the genetic code of DNA is maintained and reproduced

Archeology

A synchrotron X-ray beam at the SSRL facility illuminated an obscured work erased, written over and even painted over of the ancient mathematical genius Archimedes 287 B.C.

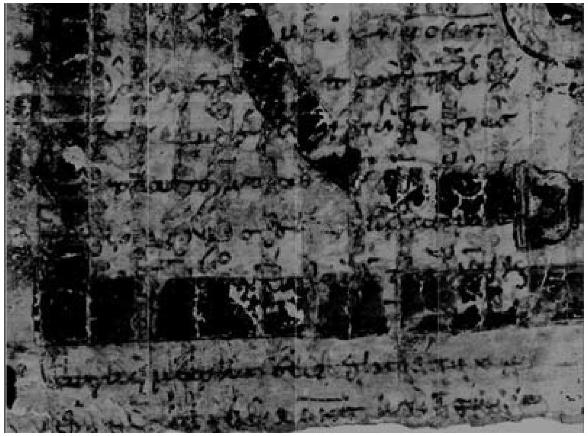

X-ray fluorescence imaging revealed the hidden text by revealing the iron contained in the ink used by a 10th century scribe. This X-ray image shows the lower left corner of the page.

Protein Crystallography

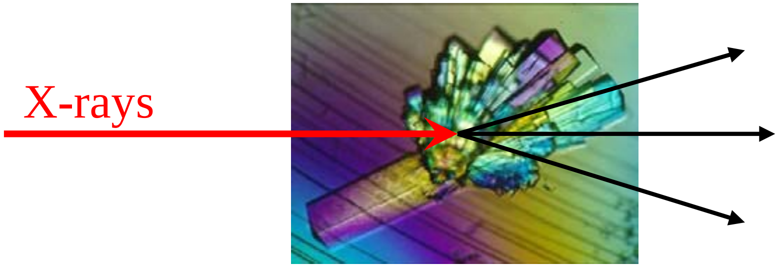

Protein crystal

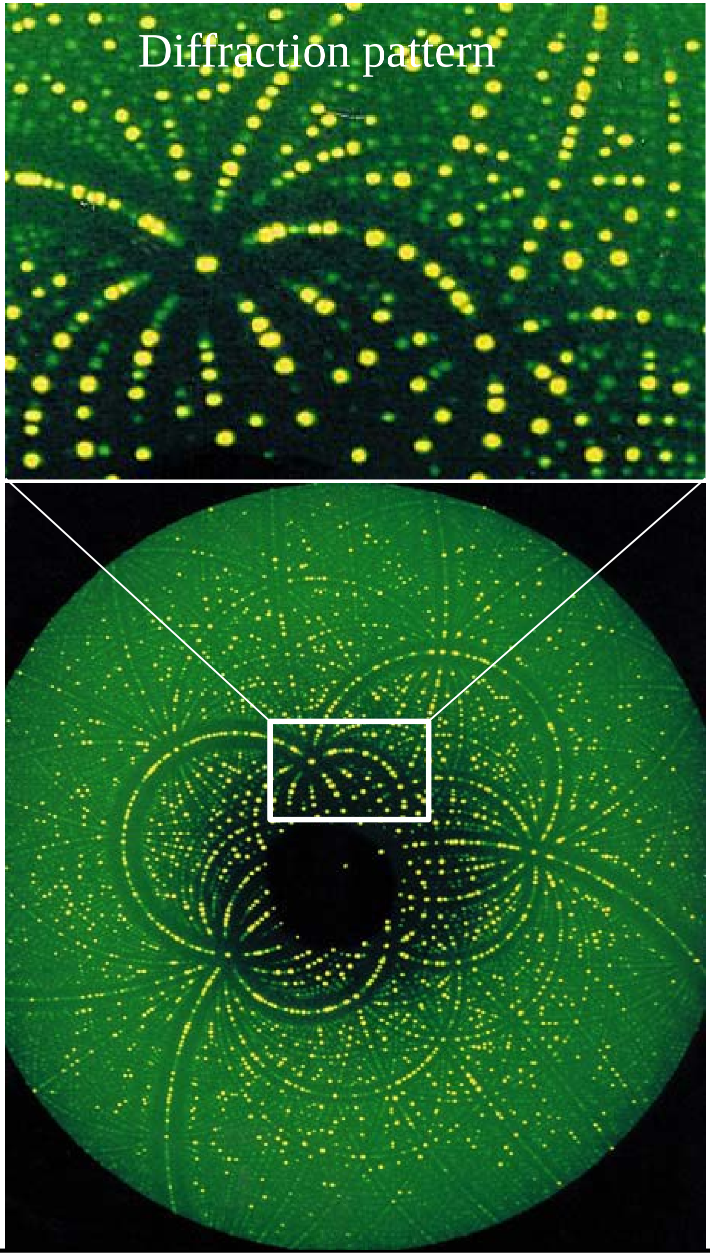

Bragg Scattering in Crystals

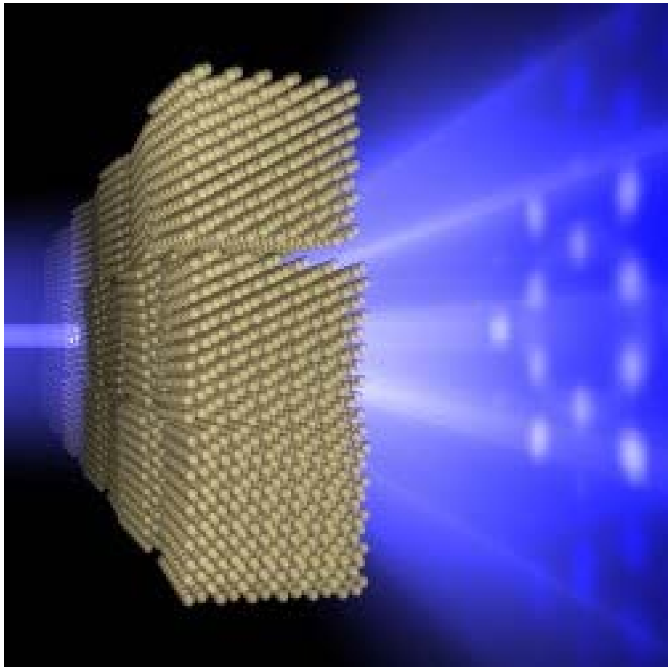

- Regular structure (crystal)
- Monochromatic light

⇒ Diffractive Pattern

Imaging of magnetic domains

Circularly polarized SR,
E = 778 eV

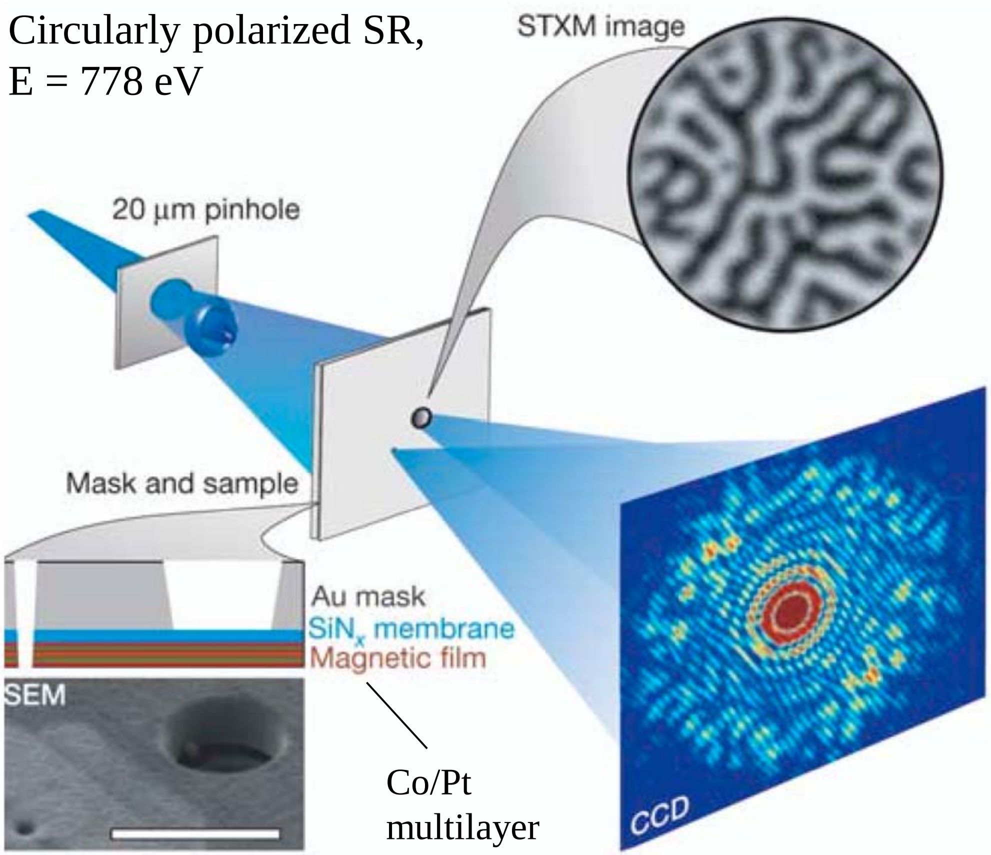

Lensless imaging of magnetic nanostructures by X-ray spectro-holography

S. Eisebitt[1], J. Lüning[2], W. F. Schlotter[2,3], M. Lörgen[1], O. Hellwig[1,4], W. Eberhardt[1] & J. Stöhr[2]

[1]BESSY mbH, Albert-Einstein-Straße 15, 12489 Berlin, Germany
[2]SSRL, Stanford Linear Accelerator Center, 2575 Sand Hill Road, Menlo Park, California 94025, USA
[3]Department of Applied Physics, 316 Via Pueblo Mall, Stanford University, Stanford, California 94305-4090, USA
[4]San Jose Research Center, Hitachi Global Storage Technologies, 650 Harry Road, San Jose, California 95120, USA

Nature 432, 885 (2004)

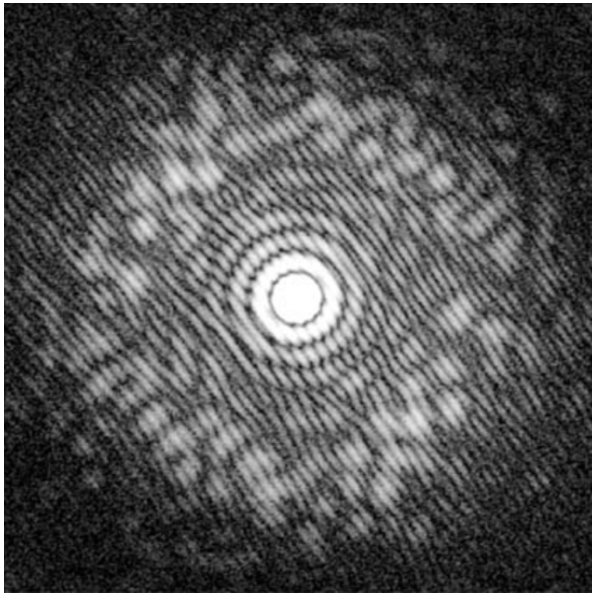

Microstructure of bones: Development during Osteoporosis disease

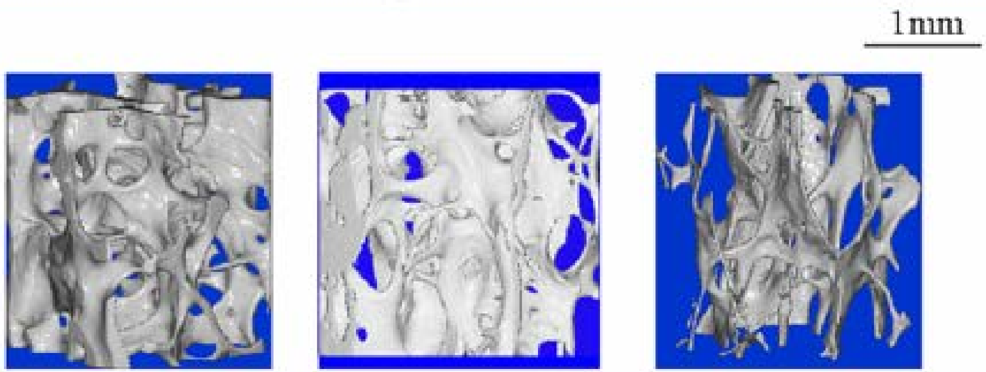

33 years 55 years 63 years

Microstructure of ice crystals in snow

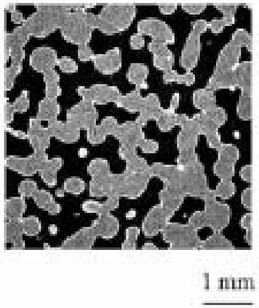

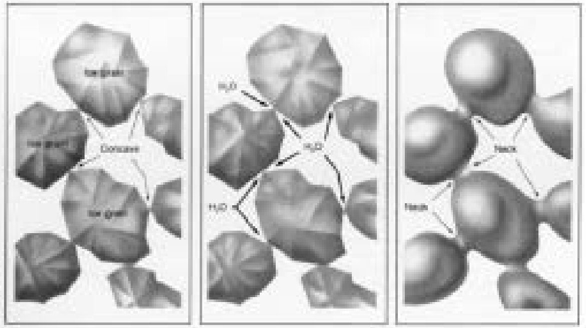

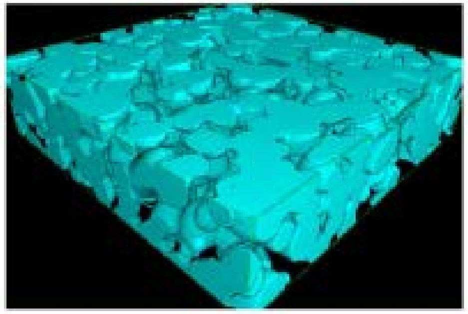

Structure of wet snow

Improvement of:

Spatial resolution
Energy resolution
Time resolution

Most of present-day experiments are dealing with equilibrium properties of condensed matter. In the future, non-equilibrium properties will be of great interest:

Dynamics of phase transitions, magnetic switching phenomena, chemical reactions etc.

Reveal the underlying mechanisms by taking snapshots on ultrashort time scales!

Future experiments with Synchrotron Radiation

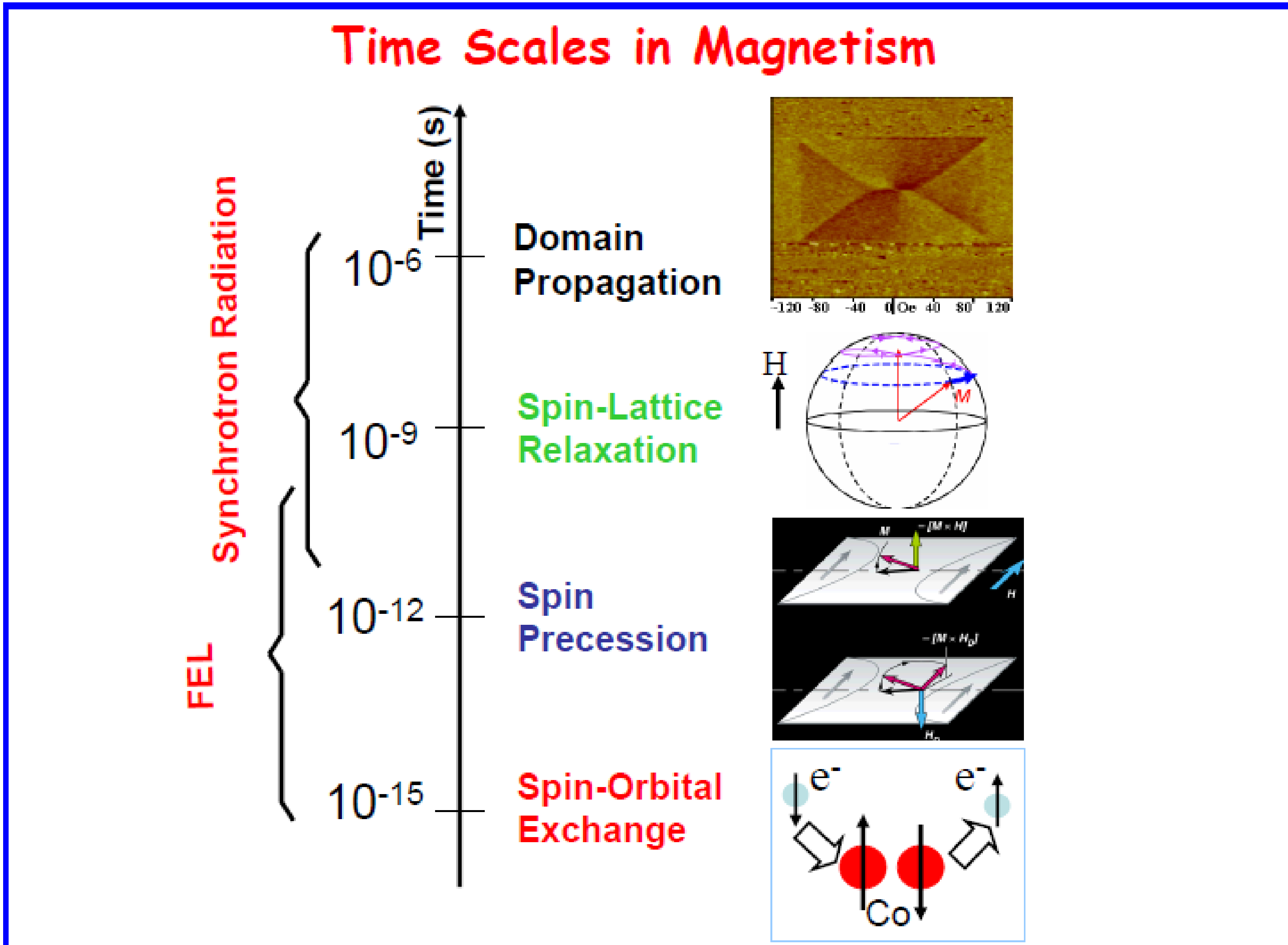

New radiation sources

Limits of Storage – Ring Based Sources

Beam properties reflect the equilibrium
Dynamics of particle in the ring, resulting from averaging over all revolutions

Particles are re-cycled

Development of New Radiation Sources

Radiation is generated by single bunches passing through an undulator

Energy – Recovery Linear Accelerator (ERL)
Sub-Picosecond Pulsed Sources (SPPS)
X-ray Free Electron Laser (XFEL)

New radiation sources

Limits of Storage – Ring Based Sources

Beam properties reflect the equilibrium
Dynamics of particle in the ring, resulting from averaging over all revolutions

Particles are re-cycled

Development of New Radiation Sources

Radiation is generated by single bunches passing through an undulator

Energy – Recovery Linear Accelerator (ERL)
Sub-Picosecond Pulsed Sources (SPPS)
X-ray Free Electron Laser (XFEL)

X-ray free electron laser

self-amplified spontaneous emission

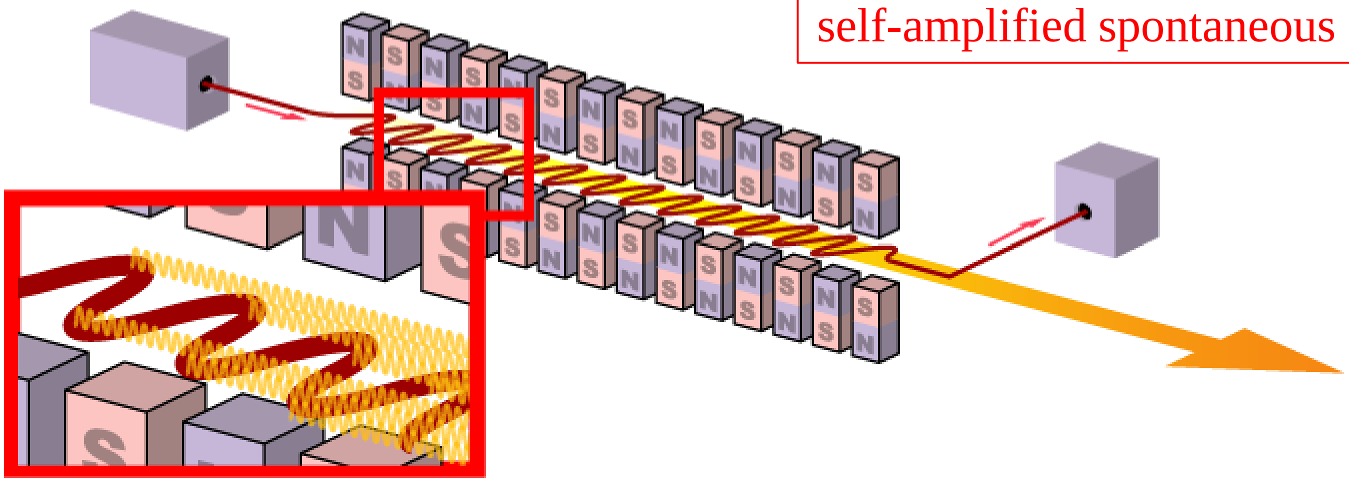

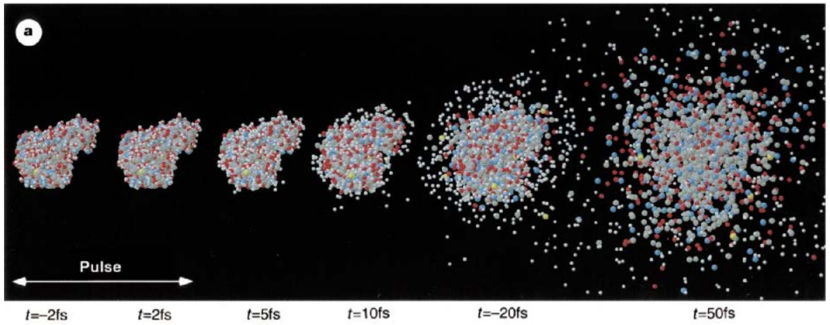

Explosion of a biomolecule (T4 lysozyme) after exposure to a 2-fs XFEL pulse (E=12 keV)

Desy XFEL

Total power received by Earth from the Sun

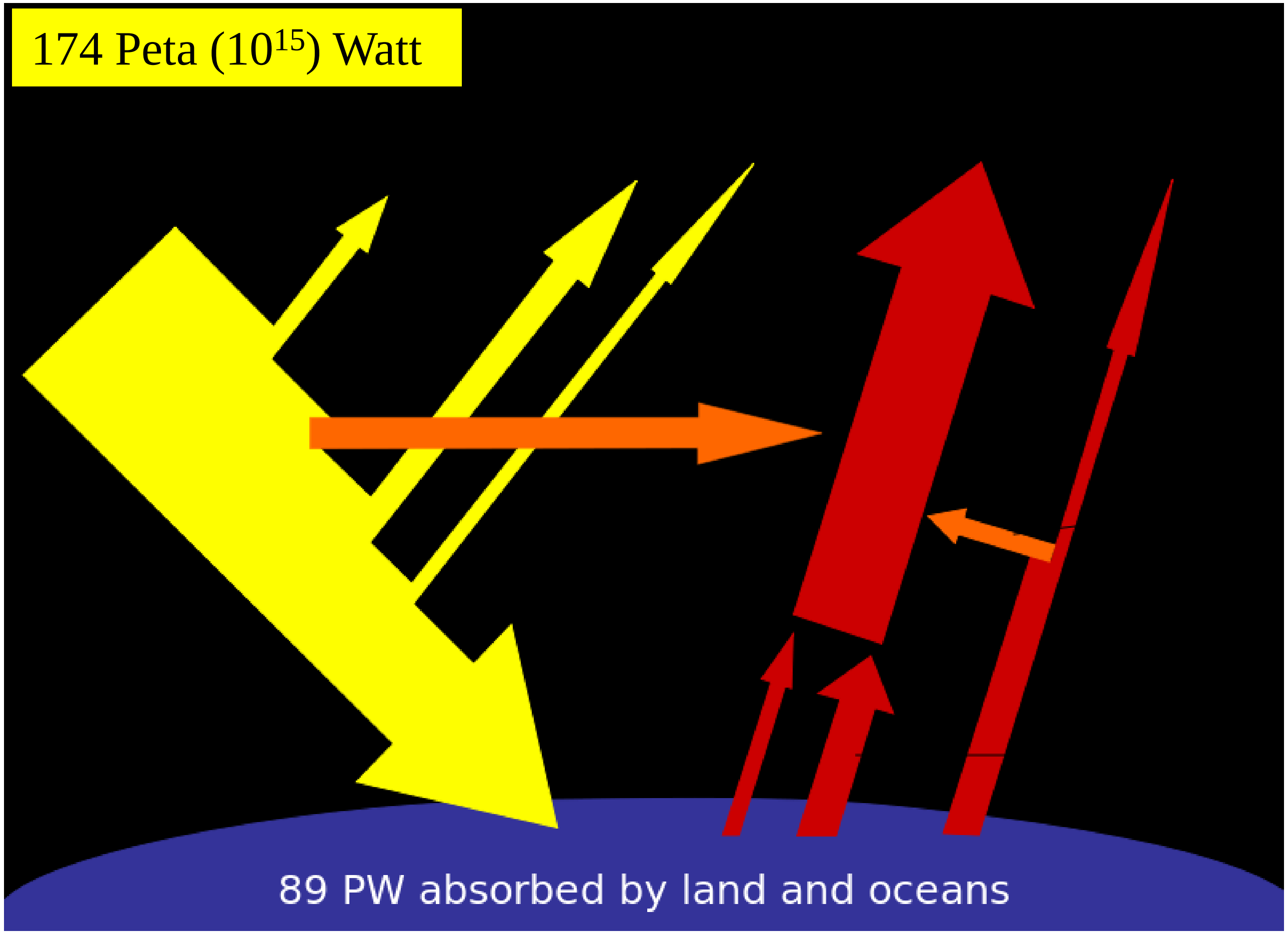

@ eli Nuclear Physics

extreme **l**ight **i**nfrastructure, Europe

Compton scattering and inverse Compton scattering

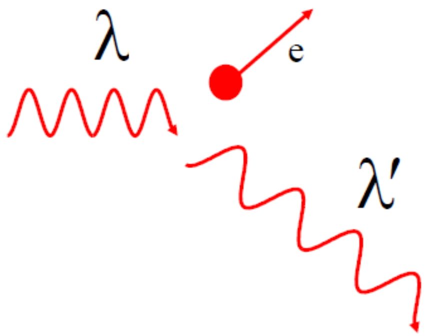

Compton scattering:

- Elastic scattering of a high-energy γ-ray on a free electron.
- **A fraction of the γ-ray energy is transferred to the electron.**
- The wave length of the scattered γ-ray is increased: λ‘ > λ.

$$h\nu \geq m_e c^2$$

$$\lambda' - \lambda = \frac{h}{m_e c} \cdot (1 - cos\theta_\gamma)$$

$$\boxed{E'_\gamma = \frac{E_\gamma}{1 + \frac{E_\gamma}{m_e c^2} \cdot (1 - cos\theta)}}$$

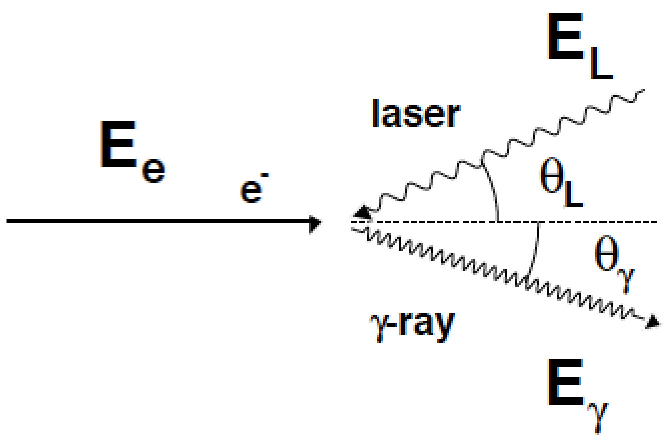

Inverse Compton scattering:

- Scattering of low energy photons on ultra-relativistic electrons.
- **Kinetic energy is transferred from the electron to the photon.**
- The wave length of the scattered γ-ray is decreased: λ‘ < λ.

$$\lambda' \approx \lambda \cdot \frac{1 - \beta \cdot cos\theta_\gamma}{1 + \beta \cdot cos\theta_L}$$

Inverse Compton scattering

- Electron is moving at relativistic velocity
- Transformation from **laboratory frame** to **reference frame of e⁻** (rest frame):
  in order to repeat the derivation for Compton scattering

$$E_\gamma = \gamma \cdot E_\gamma \cdot \underbrace{\left(1 - \frac{v}{c} cos\theta_{e^- \gamma}\right)}_{\text{Doppler shift}}$$

Lorentz factor: $\gamma = (1-\beta^2)^{-1/2} = 1 + \frac{T_e^{MeV}}{931.5 \cdot 0.00055}$

differential cross section (Klein-Nishina)

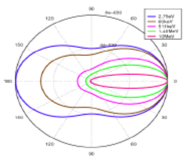

$$E'_\gamma = \frac{E_\gamma}{1 + \frac{E_\gamma}{m_e c^2} \cdot (1 - cos\phi)}$$

Compton scattering in rest frame of e⁻

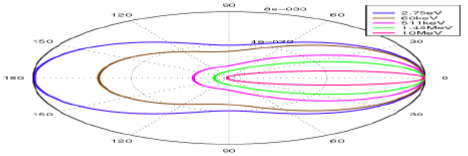

$$E'_\gamma = \gamma \cdot E'_\gamma \left(1 + \frac{v}{c} cos\theta_{e^- \gamma'}\right)$$

transformation into the laboratory frame

- Limit $E_\gamma \ll m_e c^2$

$$E'_\gamma \approx \gamma^2 \cdot E_\gamma \left(1 - \frac{v}{c} cos\theta_{e^- \gamma}\right)\left(1 + \frac{v}{c} cos\theta_{e^- \gamma'}\right)$$

$$\boxed{E'_\gamma \approx 4\gamma^2 \cdot E_\gamma}$$

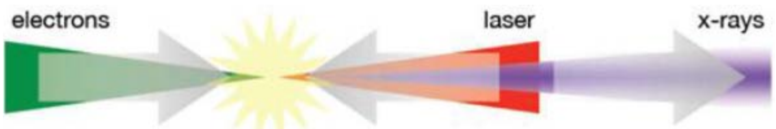

electron and γ interaction $\theta_{e^- \gamma} \sim 180^0$ γ‘ emission relative to electron $\theta_{e^- \gamma'} \sim 0^0$

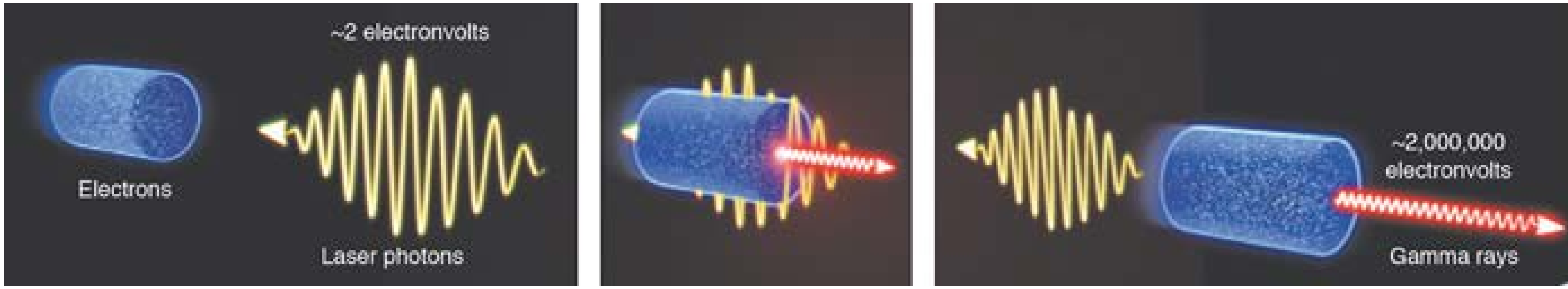

Compton recoil

Doppler upshift

$$\omega_x \simeq \frac{4\gamma_0^2}{1+\gamma_0^2\theta^2+4\gamma_0 k_0 \bar{\lambda}_c}\,\omega_\ell$$

energy-angle correlation

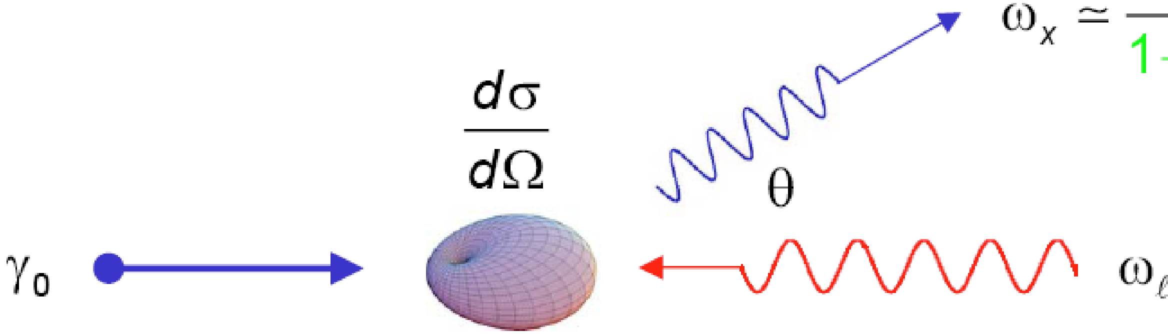

Energy – momentum conservation yields $\sim 4\gamma^2$ Doppler upshift
Thomsons scattering cross section is very small ($6\cdot 10^{-25}$ cm^2)
⇨ High photon and electron density are required

Gamma rays resulting after inverse Compton scattering

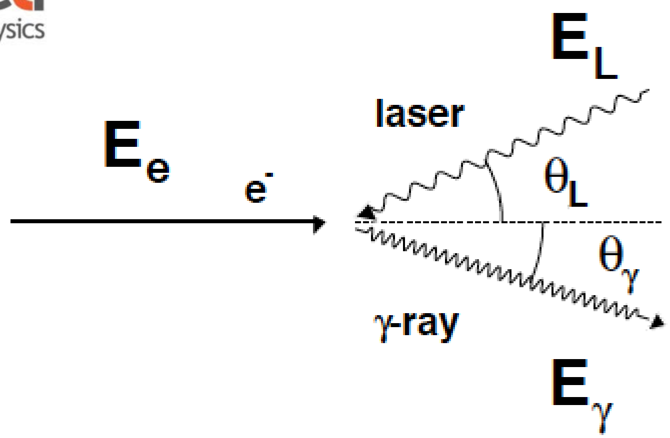

photon scattering on relativistic electrons ($\gamma >> 1$)

$h\nu = 2.3 \text{ eV} \quad (\equiv 515\ nm)$

$T_e^{lab} = 720\ MeV \quad \rightarrow \quad \gamma_e = 1 + \frac{T_e^{lab}[MeV]}{931.5 \cdot A_e[u]} = 1410$

$$\boxed{E_\gamma = 2\gamma_e^2 \frac{1 + cos\theta_L}{1 + \left(\gamma_e \theta_\gamma\right)^2 + a_0^2 + \frac{4\gamma_e E_L}{mc^2}} \cdot E_L}$$

$\frac{4\gamma_e E_L}{mc^2}$ = recoil parameter

$a_L = \frac{eE}{m\omega_L c}$ = normalized potential vector of the laser field

E = laser electric field strength $E_L = \hbar\omega_L$

$\gamma_e = \frac{E_e}{mc^2} = \frac{1}{\sqrt{1-\beta^2}}$ = Lorentz factor

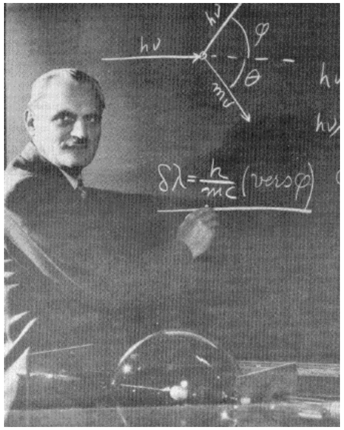

A. H. Compton
Nobel Prize 1927

maximum frequency amplification:

head-on collision ($\theta_L = 0^0$) & backscattering ($\theta_\gamma = 0^0$)

$\boxed{E_\gamma \sim 4\gamma_e^2 \cdot E_L}$ $\quad \cong 18.3\ MeV$

Scattered photons in collision

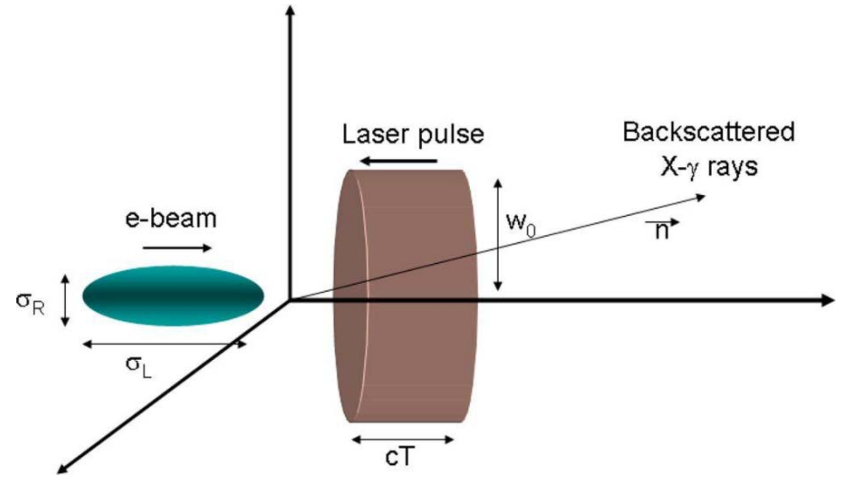

Yb: Yag J-class laser

10 Peta (10^{15}) Watt

$Q = 1[nC]$ $\quad U_L = 0.5[J]$ $\quad h\nu_L = 2.4[eV] = 3.86 \cdot 10^{-19}[J] \equiv 515[nm]$

$\rightarrow N_e = 6.25 \cdot 10^9$ $\quad \rightarrow N_L = 1.3 \cdot 10^{18}$

$\boxed{\text{Luminosity:} \quad L = \frac{N_L \cdot N_e}{4\pi \cdot \sigma_R^2} \cdot f}$ $\cong 2.9 \cdot 10^{32} \cdot f \ [cm^{-2}s^{-1}]$ $\qquad \sigma_R = 15[\mu m]$

$\boxed{\gamma\text{-ray rate:} \quad N_\gamma = L \cdot \sigma_{Thomson}}$ $\cong 2 \cdot 10^8 \cdot f \ [s^{-1}]$ $\qquad \sigma_T = 0.67 \cdot 10^{-24}[cm^2]$

(full spectrum)

repetition rate:
$f = 3.2 \ kHz$

Thomson Scattering

J. J. Thomson
Nobel prize 1906

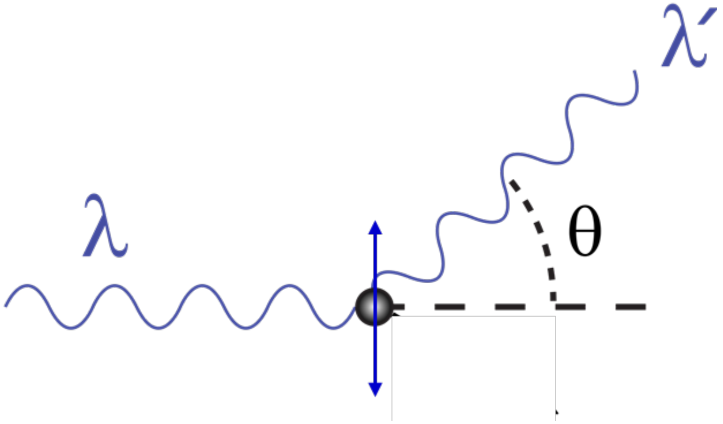

Thomson scattering = elastic scattering of electromagnetic radiation by an electron at rest

– the electric and magnetic components of the incident wave act on the electron
– the electron acceleration is mainly due to the electric field

→ the electron will move in the direction of the oscillating electric field
→ the moving electron will radiate electromagnetic dipole radiation
→ the radiation is emitted mostly in a direction perpendicular to the motion of the electron
→ the radiation will be polarized in a direction along the electron motion

Thomson Scattering

J. J. Thomson
Nobel prize 1906

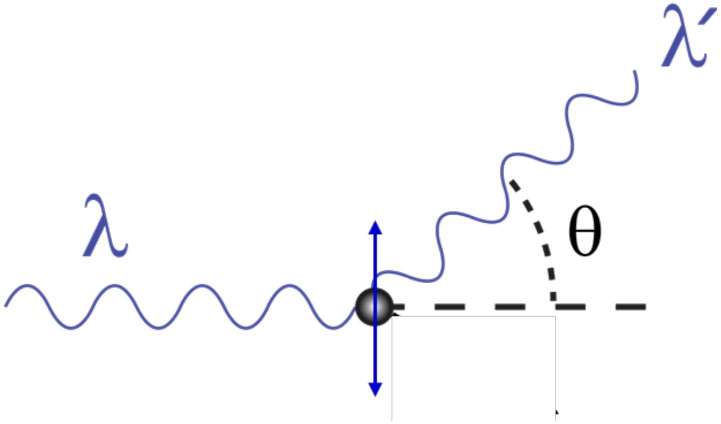

$$\frac{d\sigma_T(\theta)}{d\Omega} = \frac{1}{2} r_0^2 \cdot (1 + cos^2\theta)$$ differential cross section

$$r_0 = \frac{e^2}{4\pi\varepsilon_0 m_e c^2} = 2.818 \cdot 10^{-15}\ [m]$$ classical electron radius

$$\sigma_T = \int \frac{d\sigma_T(\theta)}{d\Omega} d\Omega = \frac{2\pi r_0^2}{2} \int_0^\pi (1 + cos^2\theta) d\theta = \frac{8\pi}{3} r_0^2 = 6.65 \cdot 10^{-29}\ [m^2] = 0.665\ [b]$$

Scattered photons in collision

$$E_\gamma = 2\gamma_e^2 \frac{1 + cos\theta_L}{1 + \left(\gamma_e \theta_\gamma\right)^2 + a_0^2 + \frac{4\gamma_e E_L}{mc^2}} \cdot E_L$$

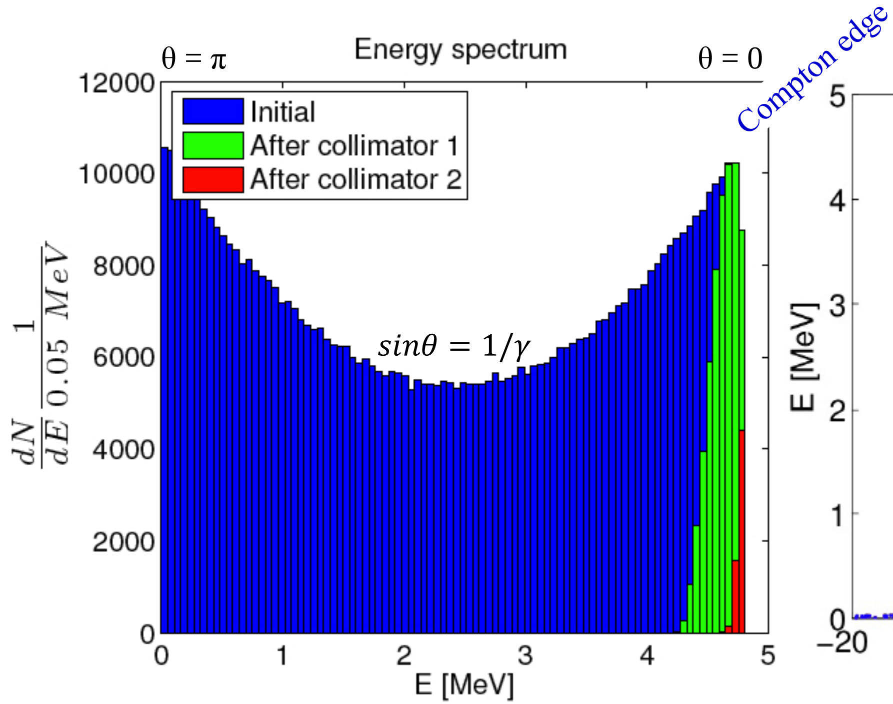

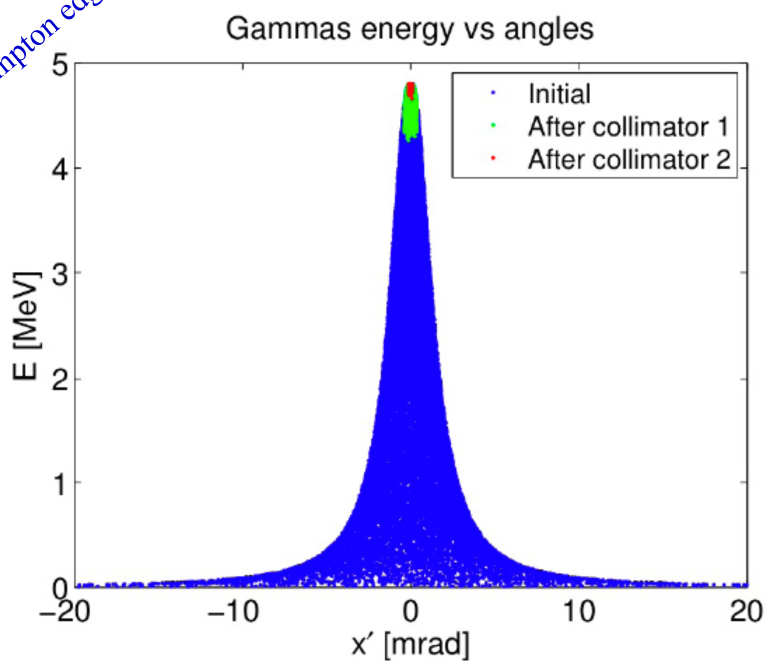

Photon extraction line

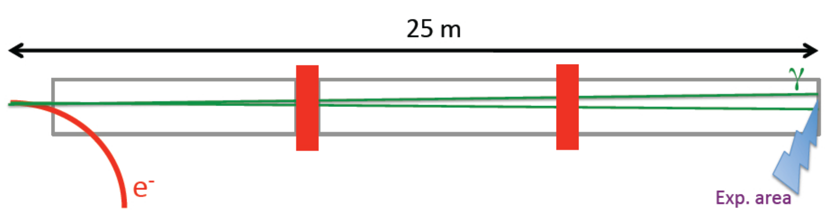

- Collimator 1 : d=11 m r= 0.3 cm , t= 5 cm (W)
- Collimator 2 : d=15 m r= 0.1 cm, t= 5 cm (W)

Inverse Compton scattering of laser light

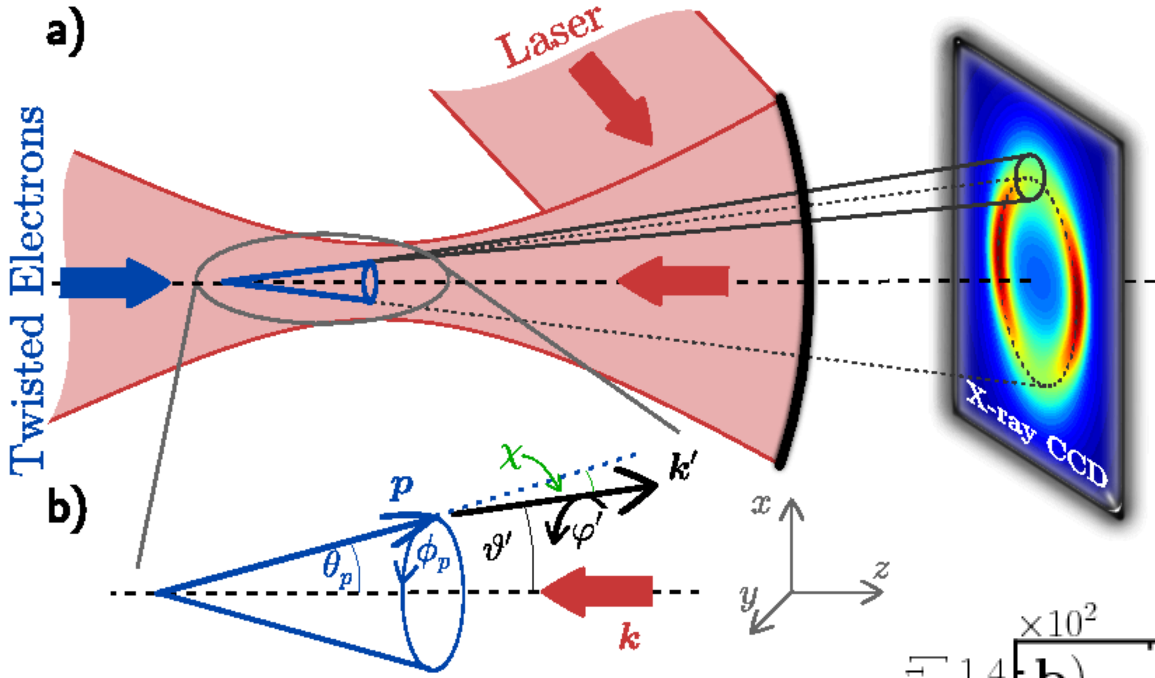

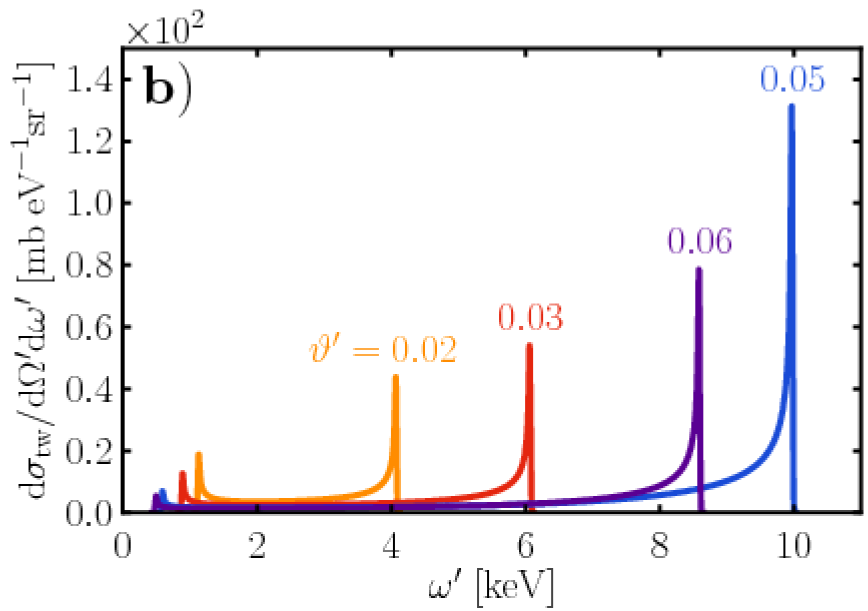

Extreme Light Infrastructure – Nuclear Physics

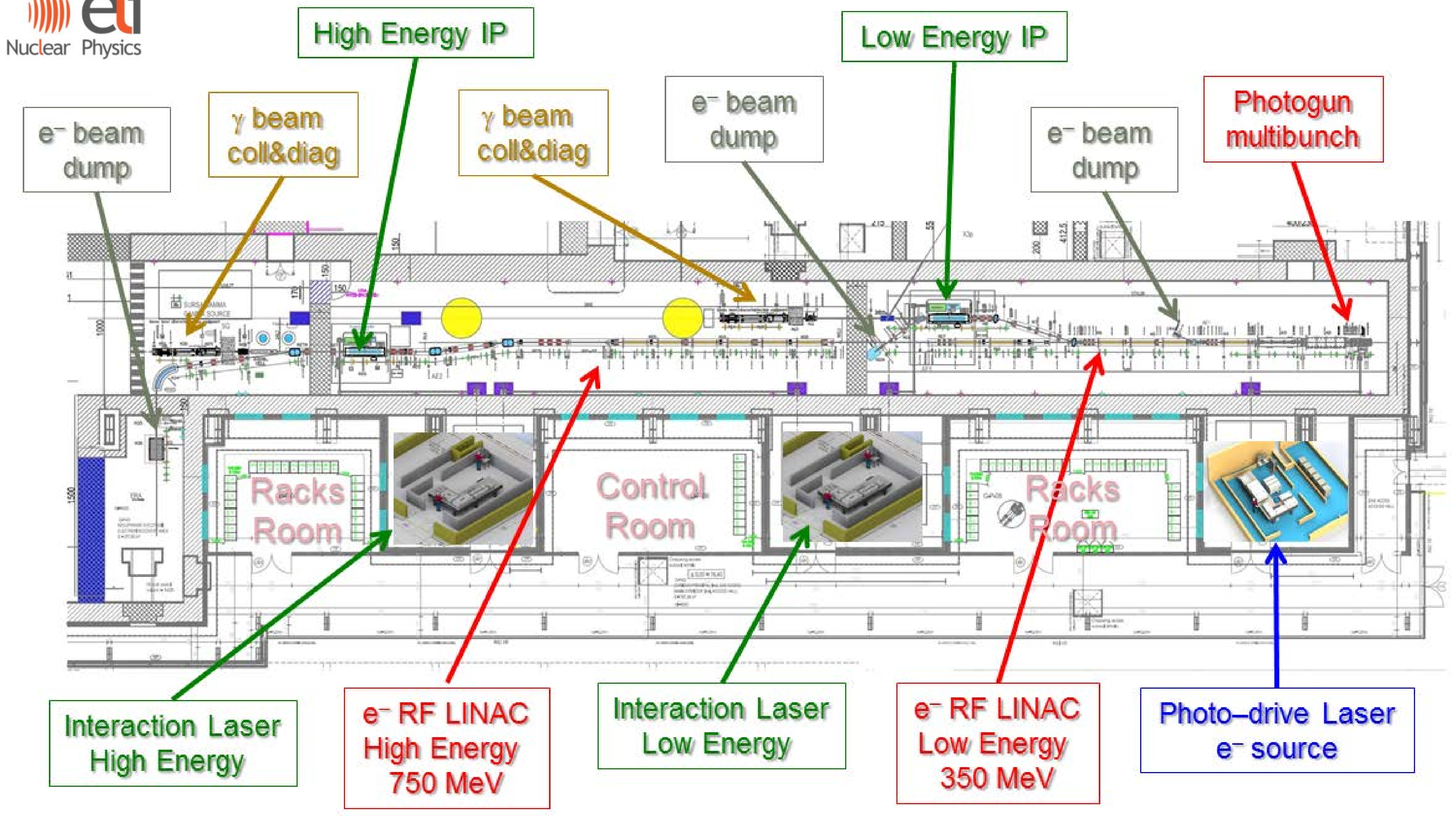

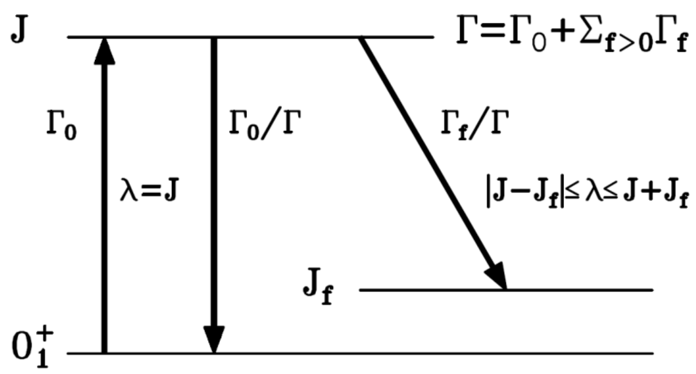

- Widths of particle-bound states: $\Gamma \lesssim 10eV$

- Breit-Wigner absorption resonance curve for isolated resonance:

$$\sigma_a(E) = \pi\bar{\lambda}^2 \frac{2J+1}{2} \frac{\Gamma_0\Gamma}{(E-E_r)^2+(\Gamma/2)^2} \sim \Gamma_0/\Gamma$$

- Resonance cross section can be very large: $\sigma_0 \cong 200\ [b]$ (for $\Gamma_0 = \Gamma$, 5 MeV)

- Example: 10 mg, A~200 → $N_{target} = 3\cdot 10^{19}$, $N_\gamma = 100$, event rate = 0.6 [s^{-1}]

Nuclear Resonance Fluorescence

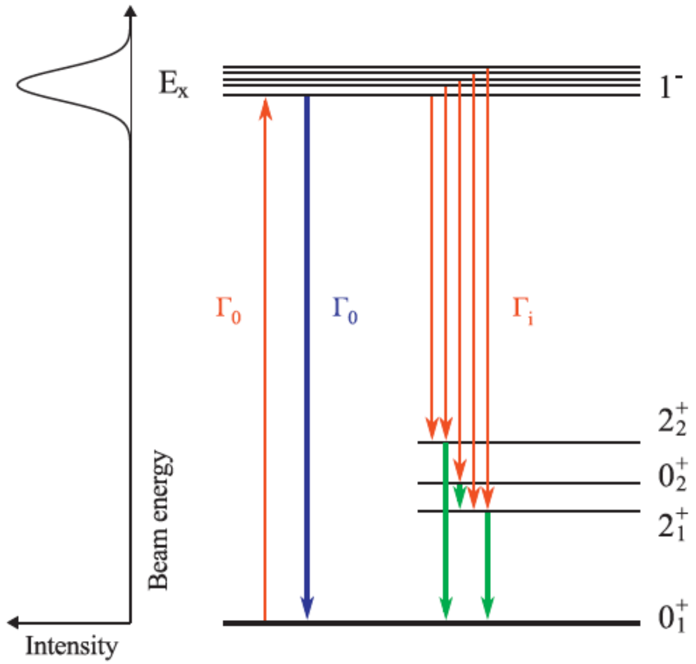

Count rate estimate
- 10^4 γ/(s eV) in 100 macro pulses
- 100 γ/(s eV) per macro pulse
- example: 10 mg, A ~ 200 target
- resonance width Γ = 1 eV
- 2 excitations per macro pulse
- 0.6 photons per macro pulse in detector
- pp-count rate 6 Hz
- 1000 counts per 3 min

❖ narrow band width 0.5%

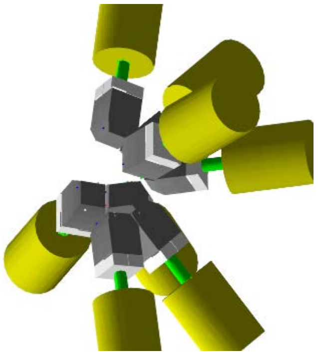

8 HPGe detectors
2 rings at 90^0 and 127^0
ε_{rel}(HPGe) = 100%
solid angle ~ 1%
photopeak ε_{pp} ~ 3%

Nuclear Resonance Fluorescence

❖ narrow bandwidth allows selective excitation and detection of decay channels

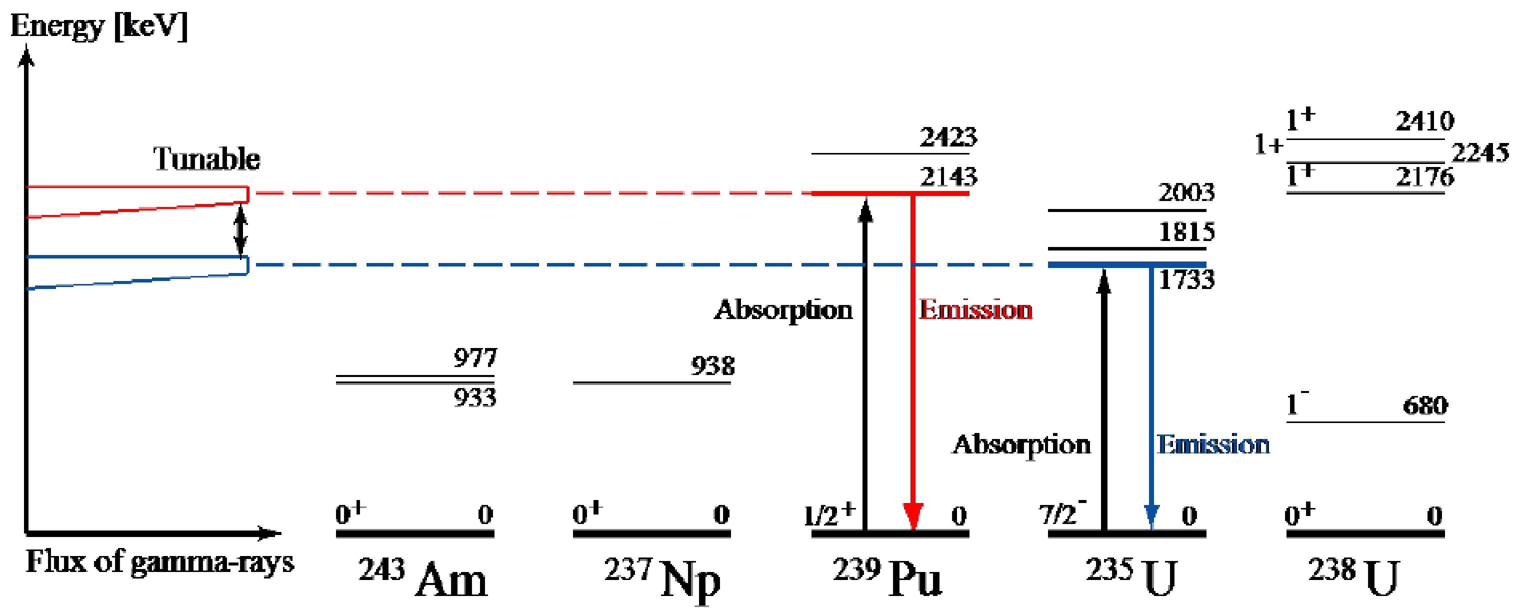

❖ **Decay to intrinsic excitations**